Electron-Deficient Group 4 Metal Complexes of Sulfur-Bridged Dialkoxide Ligands: Synthesis, Structure, and Polymerization Activity Studies

Laurent Lavanant,[†] Anca Silvestru,[†] Anne Faucheux,[†] Loic Toupet,[‡] Richard F. Jordan,[§] and Jean-François Carpentier*[,†]

Organométalliques et Catalyse, UMR 6509 CNRS-Université de Rennes 1, Institut de Chimie de Rennes, 35042 Rennes Cedex, France, Groupe Matière Condensée et Matériaux, Cristallochimie, UMR 6626 CNRS-Université de Rennes 1, 35042 Rennes Cedex, France, and Department of Chemistry, The University of Chicago, 5735 S. Ellis Avenue, Chicago, Illinois 60637

Received July 6, 2005

Coordination of the sulfur-bridged dialkoxide ligands $\{OCR_2CH_2SCH_2CR_2O\}^{2-}$ ($\{OSOR\}^{2-}$, R = Me, *p*-tolyl) on titanium and zirconium centers has been studied. A variety of complexes having one or two ancillary $\{OSO^{Me}\}^{2-}$ ligands, viz., $M(OR)_2\{OSO^{Me}\}$ (M = Zr, OR = O*t*Bu, **4**; M = Ti, OR = O*i*Pr, **5**), $M\{OSO^{Me}\}_2$ (M = Zr, **6**; Ti, **7**), $Zr(CH_2Ph)_2\{OSO^{Me}\}$ (**8**), and $MCl_2\{OSO^{Me}\}(THF)_n$ (M = Zr, *n* = 0, **9**; *n* = 1, **10**; *n* = 2, **11**; M = Ti, *n* = 0, **12**; *n* = 2, **13**), have been prepared in good yields by alcohol or alkane elimination from $\{OSO^{Me}\}H_2$ (**1a**) or by salt metathesis routes from alkali metal salts $M\{OSO^{Me}\}$ (M = K, **2a**; M = Li, in situ-generated). Coordination of the *p*-tolyl-substituted ligand by these and other routes proved to be much more difficult, and only $TiCl_2\{OSO^{tol}\}$ (**14**) was obtained. Crystallographic studies showed that dichloro complexes **11** and **13** and bis-ligand complex **7** adopt in the solid state mononuclear structures with no bonding interaction between the sulfur atom and metal centers. The crystal structure of **4** contains two independent dinuclear molecules that interconvert formally by exchange of *t*BuO and chelating $\{OSO^{Me}\}$ ligands between terminal and bridging modes and feature normal Zr−S bonds. NMR data for **4** and **12** are consistent with dinuclear C_1-symmetric structures in toluene solution, while dibenzyl complex **8** has a mononuclear structure. Variable-temperature NMR studies combined with line-shape analysis established that the fluxional behavior of **8** results from the exchange between η^2/η^1-benzyl ligands ($\Delta H^{\ddagger} = 10.6 \pm 1$ kcal·mol^{-1}; $\Delta S^{\ddagger} = -2.7 \pm 2$ cal·mol^{-1}·K^{-1}). Abstraction of one benzyl ligand of **4** with 1 equiv of $[Ph_3C][B(C_6F_5)_4]$ or $B(C_6F_5)_3$ proceeds cleanly to give the corresponding thermally unstable, ionic species $[Zr(CH_2Ph)\{OSO^{Me}\}]^+[BX(C_6F_5)_3]^-$ (X = C_6F_5, **15**; CH_2Ph, **16**), which have been characterized by ^1H, ^{11}B, ^{13}C, and ^{19}F NMR spectroscopy and show C_s symmetry in solution. The decomposition of **16** proceeds via C_6F_5/benzyl exchange from Zr to B and generates the stable $[Zr(C_6F_5)\{OSO^{Me}\}]^+[\eta^6\text{-}(PhCH_2)B(CH_2Ph)(C_6F_5)_2]^-$ (**17**). Cationic species in situ-generated from Zr chloro complexes and MAO are highly active but very unstable ethylene polymerization catalysts.

Introduction

Largely because of the search for new-generation olefin polymerization catalysts, investigation into the use of alkoxide (O-C(sp^3)) and aryloxide (O-C(sp^2)) ancillary ligands to replace the ubiquitous cyclopentadienyl-type ligands in organo group 4 metal complexes has become popular in recent years.[1] While the synthetic organometallic chemistry and catalytic applications of group 4 metal complexes of chelating bis-*aryloxide* ligands have been extensively explored,[2] the chemistry of *alkoxide*-based complexes proved to be more complicated.[3] This is inherent to the high tendency of the relatively more basic alkoxide ligands to act as bridging ligands, resulting in di- or polynuclear structures.[3] This difficulty can be partly overcome by (i) increasing the steric bulk of the −OR moieties, which is easy due to

* Corresponding author. Fax: (+33)(0)223-236-939. E-mail: jean-francois.carpentier@univ-rennes1.fr.
† Organométalliques et Catalyse, UMR 6509 CNRS.
‡ Groupe Matière Condensée et Matériaux, Cristallochimie, UMR 6626 CNRS.
§ The University of Chicago.

(1) For reviews on post-metallocene complexes of group 4 metals, see: (a) Britovsek, G. J. P.; Gibson, V. C.; Wass, D. F. *Angew. Chem., Int. Ed.* **1999**, *38*, 428−447. (b) Coates, G. W. *J. Chem. Soc., Dalton Trans.* **2002**, 467−475. (c) Gibson, V. C.; Spitzmesser, S. K. *Chem. Rev.* **2003**, *103*, 283−315. (d) Suzuki, Y.; Terao, H.; Fujita, T. *Bull. Chem. Soc. Jpn*. **2003**, *76*, 1493−1517. (e) Corradini, P.; Guerra, G.; Cavallo, L. *Acc. Chem. Res.* **2004**, *37*, 231−241.

(2) For examples in group 4 chemistry see: (a) Van der Linden, A.; Schaverien, C. J.; Meiboom, N.; Ganter, C.; Orpen, A. G. *J. Am. Chem. Soc.* **1995**, *117*, 3008−3021. (b) Tshuva, E. Y.; Goldberg, I.; Kol, M. *J. Am. Chem. Soc.* **2000**, *122*, 10706−10707. (c) Balsells, J.; Carroll, P. J.; Walsh, P. J. *Inorg. Chem.* **2001**, *40*, 5568−5574. (d) Tian, J. P.; Hustad, D.; Coates, G. W. *J. Am. Chem. Soc.* **2001**, *123*, 5134−5135.

(3) (a) Bradley, D. C.; Mehrotra, R. M.; Rothwell, I. P.; Singh, A. *Alkoxo and Aryloxo Derivatives of Metals*; Academic Press: London, 2001. (b) Mehrotra, R. M.; Singh, A. *Prog. Inorg. Chem.* **1997**, *46*, 239−545. (c) Hubert-Pfalzgraf, L. G. *Coord. Chem. Rev.* **1998**, *178*−*180*, 967−997.

10.1021/om050560c CCC: $30.25
Publication on Web 09/23/2005

the large availability of alcohols, or (ii) modifying the alkoxide ligand with additional donor functionalities.[3] Several group 4 metal complexes based on tridentate and tetradentate bis-aryloxide[2] and bis-alkoxide[4−7] ligands having additional coordinating heteroatom(s) (*N*, *O*, *S*) have been described. Of special interest are ligands having a sulfur bridge,[2a,8−10] since the soft sulfur atom may interact weakly with the hard metal center, possibly stabilizing a reactive cationic metal center without deactivating it, as a better donor atom would do. Theoretical computations predicted that TiMe{(2-C_6H_4O)X(2′-C_6H_4O)}$^+$ (X = O, S, Se, Te) systems act as "breathing catalysts", with the X heteroatom moving in and out from the metal center as the electron density changes, leading to a less stabilized π-olefin complex and a lower activation (ethylene insertion) barrier.[11] This effect has been proposed to account for the higher ethylene polymerization activity of some titanium sulfur-bridged bis-*aryloxide* systems as compared to methylene-bridged or directly bridged analogues.[2a,12] Predictive computational work also suggested the possible appropriateness of sulfur-bridged bis-*alkoxide* ligands of the type $\{OC_2H_2SC_2H_2O\}^{2-}$.

In this contribution, we describe the coordination chemistry of titanium(IV) and zirconium(IV) complexes of the tridentate ligand systems $\{OCR_2CH_2SCH_2CR_2O\}^{2-}$ ($\{OSOR\}^{2-}$, R = Me, *p*-tolyl). The objectives of this work were to define the $\{OSOR\}^{2-}$ coordination properties in simple group 4 $MX_2\{OSOR\}$ complexes, to prepare $MR_2\{OSOR\}$ and also $[M(R)\{OSOR\}]^+$ alkyl species, and to explore the ethylene polymerization properties of $MX_2\{OSOR\}$/MAO and $[M(R)\{OSOR\}]^+$ catalysts.

Results and Discussion

Ligands Synthesis. Two ligands were prepared to explore the influence of the R substituents in $\{OCR_2CH_2SCH_2CR_2O\}^{2-}$ ligands and Ti(IV) and Zr(IV) complexes thereof. The known dimethyl-substituted sulfur-bridged diol $\{OSOMe\}H_2$ (**1a**)[13] and the new *para*-tolyl-substituted diol $\{OSO^{tol}\}H_2$ (**1b**) were prepared in good yields by the reaction of sodium sulfide with the corresponding tertiary chlorhydrine in boiling ethanol (eq 1). Diol **1a** was readily obtained in pure, dry form. However, **1b** was isolated by recrystallization as the mono-water adduct, as evidenced by elemental analysis and a single X-ray diffraction study (Figure 1, Table 1). Treatment of **1b** with drying agents ($MgSO_4$, MS 4 Å, etc.) for long periods did not remove the water. The strong interaction of water with **1b** can be correlated with the extensive hydrogen bonding in the solid state (Figure 2). The higher acidity of $-CAr_2OH$ (pK_a = ca. 13.5) as compared to $-CMe_2OH$ (pK_a = ca. 15.3)[14] makes **1b** a better H-bond donor and presumably accounts for the formation of the robust water adduct **1b**·H_2O.

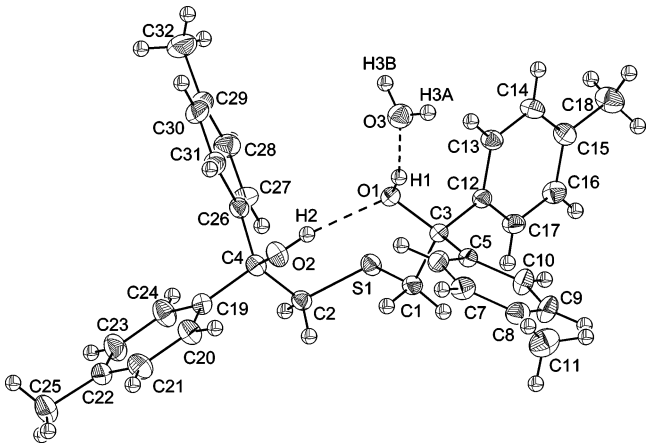

Figure 1. ORTEP drawing of $\{OSO^{tol}\}H_2$ (**1b**). Ellipsoids are drawn at the 50% probability level.

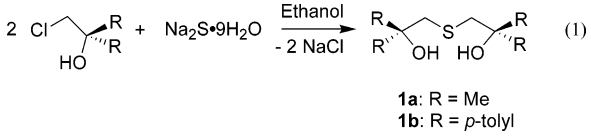

Diols **1a** and **1b** were transformed into the corresponding dipotassium salts (eq 2). Treatment of **1a** with potassium in THF at room temperature gave $K_2\{OSO^{Me}\}$ (**2a**) in 94% yield. This procedure was not effective for **1b**, but $K_2\{OSO^{tol}\}$ (**2b**) could be isolated in 35% yield by reaction of **1b** with potassium *tert*-butoxide.

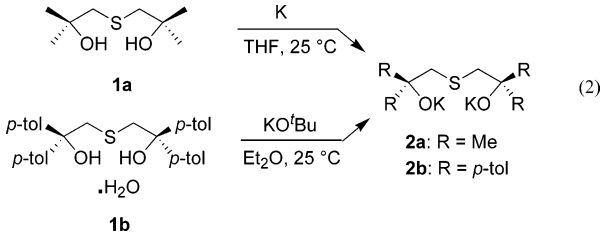

The trimethylsilyl ethers $\{OSO^R\}(TMS)_2$ (**3a**,**b**) were prepared in high yield by reaction of **1a**,**b** with

(4) Shao, P.; Gendron, R. A. L.; Berg, D. J.; Bushnell, G. W. *Organometallics* **2000**, *19*, 509−520.

(5) Gauvin, R. M.; Osborn, J. A.; Kress, J. *Organometallics* **2000**, *19*, 2944−2946.

(6) (a) Manickam, G.; Sundararajan, G. *Tetrahedron: Asymmetry* **1999**, *10*, 2913−2925. (b) Mack, H.; Eisen, M. *J. Chem. Soc., Dalton Trans.* **1998**, 917−921.

(7) Related group 4 amino-dialkoxide complexes derived from the parent N-bridged ligand system $[OCR_2CH_2N(CH_2Ph)CH_2CR_2O]^{2-}$ ($[ONO^R]^{2-}$, R = Me, *p*-tolyl) have also been prepared. Lavanant, L.; Toupet, L.; Lehmann, C. W.; Carpentier, J.-F. *Organometallics* **2005**, accepted for publication.

(8) (a) Kakugo, M.; Miyatake, T.; Mizunuma, K. *Chem. Express.* **1987**, *2*, 445−448. (b) Miyatake, T.; Mizunuma, K.; Seki, Y.; Kakugo, M. *Macromol. Chem., Rapid Commun.* **1989**, *10*, 349−352. (c) Miyatake, T.; Mizunuma, K.; Kakugo, M. *Makromol. Chem., Macromol. Symp.* **1993**, *66*, 203−214.

(9) (a) Fokken, S.; Spaniol, T. P.; Kang, H.-C.; Massa, W.; Okuda, J. *Organometallics* **1996**, *15*, 5069−5072. (b) Sernetz, F. G.; Muelhaupt, R.; Fokken, S.; Okuda, J. *Macromolecules* **1997**, *30*, 1562−1569. (c) Capacchione, C.; Proto, A.; Ebeling, H.; Mülhaupt, R.; Möller, K.; Spaniol, T. P.; Okuda, J. *J. Am. Chem. Soc.* **2003**, *125*, 4964−4965. (d) Fokken, S.; Reichwald, F.; Spaniol, T. P.; Okuda, J. *J. Organomet. Chem.* **2002**, *663*, 158−163. (e) Natrajan, L. S.; Wilson, C.; Okuda, J.; Arnold, P. L. *Eur. J. Inorg. Chem.* **2004**, 3724−3732. (f) Capacchione, C.; Proto, A.; Okuda, J. *J. Polym. Sci. A: Polym. Chem.* **2004**, *42*, 2815−2822. (g) Capacchione, C.; Manivannan, R.; Barone, M.; Beckerle, K.; Centore, R.; Oliva, L.; Proto, A.; Tuzi, A.; Spaniol, T. P.; Okuda, J. *Organometallics* **2005**, *24*, 2971−2982.

(10) (a) Takashima, Y.; Nakayama, Y.; Hirao, T.; Yasuda, H.; Harada, A. *J. Organomet. Chem.* **2004**, *689*, 612−619. (b) Janas, S.; Jerzykiewicz, L. B.; Przybylak, K.; Sobota, P.; Sczzegot, K.; Wisniewska, D. *Eur. J. Inorg. Chem.* **2004**, 1639−1645. (c) Janas, S.; Jerzykiewicz, L. B.; Przybylak, K.; Sobota, P.; Sczzegot, K.; Wisniewska, D. *Eur. J. Inorg. Chem.* **2005**, 1063−1070. (e) Janas, Z.; Jerzykiewicz, L. B.; Sobota, P.; Sczzegot, K.; Wisniewska, D. *Organometallics* **2005**, *24*, 3987−3994.

(11) (a) Froese, R. D. J.; Musaev, D. G.; Matsubara, T.; Morokuma, K. *J. Am. Chem. Soc.* **1997**, *119*, 7190−7196. (b) Froese, R. D. J.; Musaev, D. G.; Matsubara, T.; Morokuma, K. *Organometallics* **1999**, *18*, 373−379.

Table 1. Crystal Data and Structure Refinement for 1b, 3b, 4, 7, 11, and 13

	1b	3b	4	7	11	13
formula	$C_{32}H_{36}O_3S$	$C_{38}H_{50}O_2SSi_2$	$C_{16}H_{34}O_4SZr$	$C_{16}H_{32}O_4S_2Ti$	$C_{16}H_{32}Cl_2O_4SZr$	$C_{16}H_{32}Cl_2O_4STi$
cryst size, mm	0.30 × 0.17 × 0.15	0.42 × 0.40 × 0.22	0.17 × 0.14 × 0.05	0.25 × 0.08 × 0.08	0.50 × 0.42 × 0.40	0.54 × 0.45 × 0.32
M, g·mol^{-1}	500.67	627.02	413.71	400.44	482.60	439.28
cryst syst	monoclinic	monoclinic	triclinic	monoclinic	monoclinic	monoclinic
space group	$P2_1/n$	$C2$	$P\bar{1}$	$C2/c$	$P2_1/n$	$P2_1/n$
a, Å	13.0192(11)	22.692(1)	10.3427(3)	17.718(1)	10.2494(2)	10.0684(2)
b, Å	12.2471(10)	8.3884(5)	19.0944(6)	12.194(1)	10.8080(2)	10.7817(2)
c, Å	17.7002(15)	20.4111(1)	21.5341(7)	9.611(1)	20.4758(3)	20.2383(4)
α, deg	90.00	90.00	81.6410(10)	90.00	90.00	90.00
β, deg	99.614(2)	110.821(3)	77.779(2)	94.447(3)	101.990(1)	101.938(1)
γ, deg	90.00	90.00	84.072(2)	90.00	90.00	90.00
V, Å^3	2782.6(4)	3631.5(3)	4100.6(2)	2070.2(3)	2218.73(7)	2149.44(7)
Z	4	4	8	4	4	4
D_{calc}, Mg/m^3	1.195	1.147	1.340	1.285	1.445	1.357
T, K	279(2)	110(1)	100	120(1)	110	293(2)
θ range, deg	1.81−26.37	1.84−27.49	2.91−31.00	3.34−27.49	2.07−2749	2.11−27.48
μ, mm^{-1}	0.147	0.186	0.651	0.629	0.846	0.760
no. of measd reflns	21 988	13 737	46 974	8389	24 761	31 872
no. of indep reflns	5689	4434	23 443	23 54	5032	4888
no. of reflns with $I > 2\sigma(I)$	4420	3935	13 757	1989	4883	4107
no. of params	338	390	827	106	218	218
goodness of fit	1.032	1.121	1.013	1.065	1.082	1.001
R [$I > 2\sigma(I)$]	0.0449	0.0573	0.0716	0.0487	0.0249	0.0537
R_w[2]	0.1176	0.1414	0.1497	0.1284	0.0653	0.1495
lgst diff, e·Å^{-3}	0.224	0.308	2.548	0.794	1.567	1.661

$ClSiMe_3$ (eq 3). The use of DBU, instead of the usual NEt_3, and a large excess of $ClSiMe_3$ were found to be necessary to obtain a high yield of **3b**. The identity of **3b** was confirmed by an X-ray diffraction study (Figure 3, Table 1).

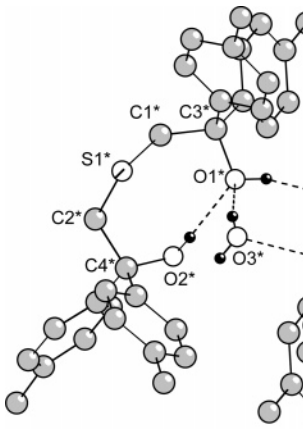

Figure 2. Hydrogen-bonding interactions involving water in the crystal structure of **1b**.

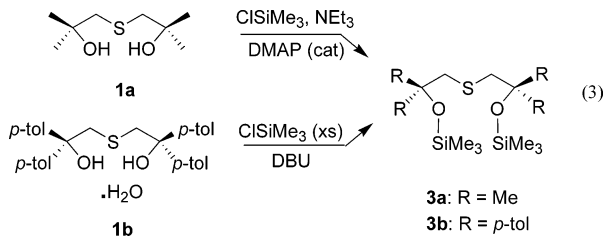

Scheme 1

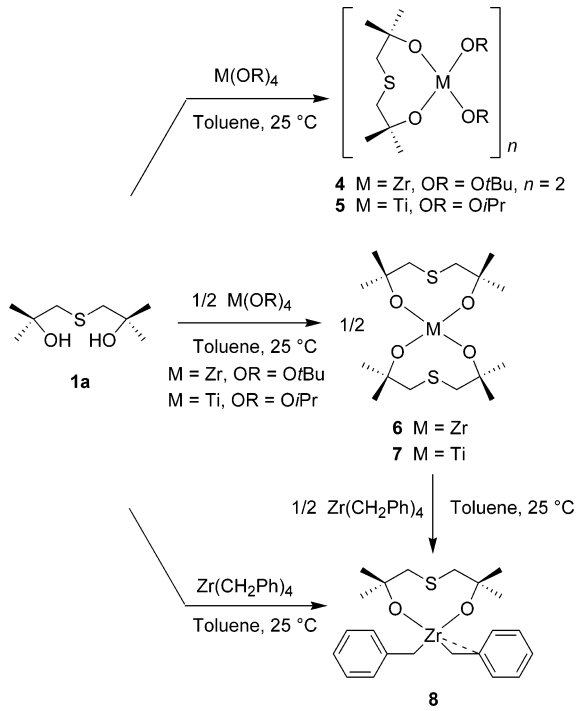

Synthesis of Neutral Complexes. Several routes to Ti-{OSO^R} and Zr-{OSO^R} complexes have been explored: (a) σ-bond metathesis reactions between the diols and an appropriate homoleptic metal precursor enabling either alkane or alcohol elimination; (b) salt elimination reactions between a alkali metal dialkoxide salt and $MCl_4(THF)_n$; (c) σ-bond metathesis reactions between the diol trimethylsilyl ethers and $MCl_4(THF)_n$. These results are summarized in Schemes 1−3. The prepared neutral complexes are all air- and moisture-sensitive and were characterized by variable-temperature ^1H and ^{13}C NMR spectroscopy, elemental analysis, and, in several cases, X-ray diffraction (vide infra).

The 1:1 σ-bond metathesis reaction of **1a** and $Zr(OtBu)_4$ proceeded readily to yield the corresponding

(12) (a) Nakayama, Y.; Watanabe, K.; Ueyama, N.; Nakamura, A.; Harada, A.; Okuda, J. *Organometallics* **2000**, *19*, 2498−2503. See also: (b) Oakes, D. C. H.; Kimberley, B. S.; Gibson, V. C.; Jones, D. J.; White, A. J. P.; Williams, D. J. *Chem. Commun.* **2004**, 2174−2175.

(13) (a) Idson, B.; Spoerri, P. E. *J. Am. Chem. Soc.* **1954**, *76*, 2902−2906. (b) Gilbert, B. C.; Larkin, J. P.; Norman, R. O. C. *J. Chem. Soc., Perkin Trans. 2* **1973**, 272−277.

(14) pK_a Values calculated with the ACD software (CambridgeSoft) for Ph_2CHOH and Me_2CHOH, respectively.

Scheme 2

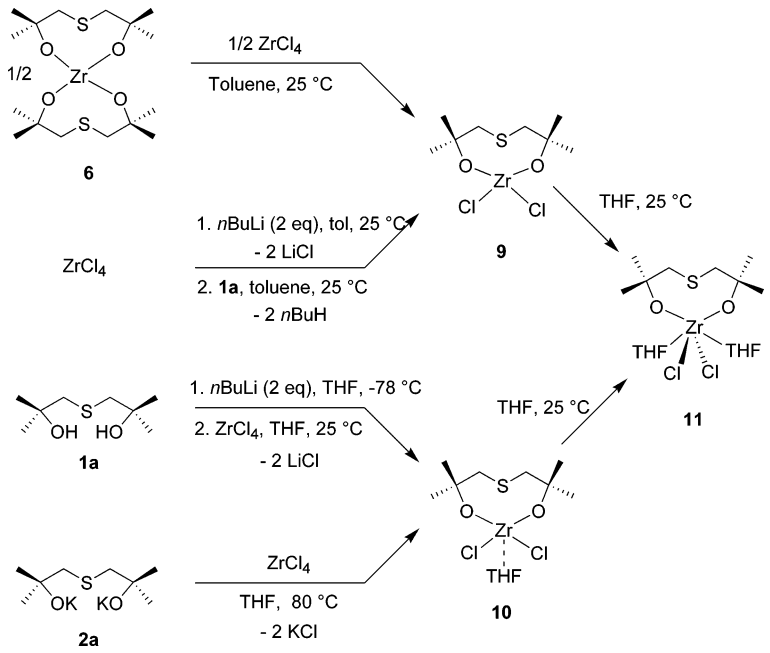

Scheme 3

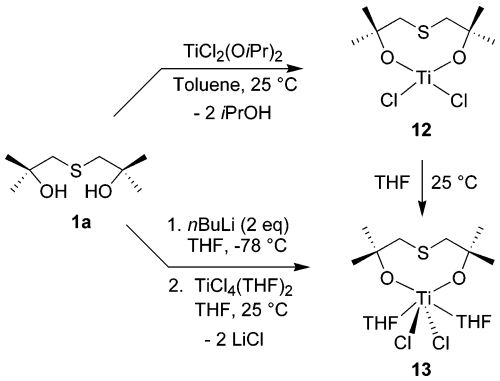

bis(*tert*-butoxide) complex **4** (Scheme 1). Attempts to perform the same reaction with Ti(O*i*Pr)$_4$ and **1a** under various conditions invariably yielded mixtures of Ti(O*i*Pr)$_2${OSO^{Me}} (**5**) and the bis-ligand complex Ti{OSO^{Me}}$_2$ (**7**), which could not be separated by recrystallization. Both **7** and the analogous Zr complex **6** were prepared efficiently by the reaction of 2 equiv of **1a** with M(OR)$_4$ complexes. Complex **6** served as an efficient entry to the dibenzyl complex Zr(CH$_2$Ph)$_2${OSO^{Me}} (**8**) via comproportionation with Zr(CH$_2$Ph)$_4$.[4] Direct alcoholysis of Zr(CH$_2$Ph)$_4$ with diol **1a** also affords **8**. However, this alkane elimination route requires careful addition at low temperature under diluted condition to avoid the formation of insoluble products. The comproportionation route is easier and more reliable.

Several ZrCl$_2${OSO^{Me}}(THF)$_n$ complexes with variable number of THF ligands (n = 0−2) were prepared as shown in Scheme 2. Comproportionation of bis-ligand complex **6** with ZrCl$_4$ in toluene gave the THF-free complex ZrCl$_2${OSO^{Me}} (**9**) in virtually quantitative yield. Complex **9** was also prepared in a one-pot procedure by first generating "Zr(nBu)$_2$Cl$_2$" from ZrCl$_4$ and nBuLi[15] and then adding 2 equiv of **1a** to perform an alkane elimination. Again, the comproportionation route proved to be easier and more efficient, although it requires two steps. Salt metathesis between ZrCl$_4$ and either the isolated dipotassium salt **2a** or in situ-generated Li$_2${OSOMe} proceeded readily in THF to give ZrCl$_2${OSO^{Me}}(THF) (**10**) with a single THF ligand. The bis-THF complex ZrCl$_2${OSO^{Me}}(THF)$_2$ (**11**) was obtained by recrystallization of **9** or **10** in THF. Complex **11** was converted to **10** upon removal of one molecule of THF by vacuum-drying for several hours.

Similarly, alcohol elimination between 2 equiv of **1a** and Ti(O*i*Pr)$_2$Cl$_2$, in situ-generated from TiCl$_4$ and Ti(O*i*Pr)$_4$,[16] gave the THF-free dichloro titanium complex **12** (Scheme 3). The elimination reaction of in situ-generated Li$_2${OSO^{Me}} with TiCl$_4$ in THF afforded the bis-THF analogue **13**. In no case could a mono-THF titanium complex be isolated.

The reactions in Schemes 1−3 were unsuccessful when carried out with *p*-tolyl-substituted diol **1b** or salts thereof. The direct reaction of **1b** with a slight excess of TiCl$_4$ in the absence of NEt$_3$[2a] did afford TiCl$_2${OSO^{tol}} (**14**), but this species could not be isolated in a pure form (eq 4). Attempts to prepare similar compounds from the reaction of TiCl$_4$(THF)$_2$ and the trimethylsilyl ether **3b** by elimination of trimethylsilyl chloride[17] were unsuccessful. The analogous dimethyl-substituted diol-ether **3a** did afford **13**, but the reactivity (maximum 15% conversion) was quite poor (eq 5).

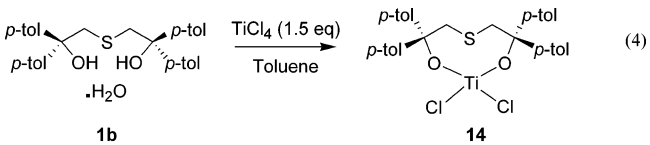

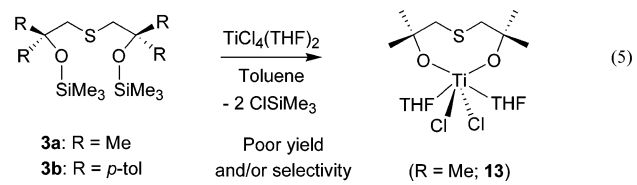

Solid-State Structures of Neutral Complexes. The solid-state structures of **4**, **7**, **11**, and **13** were

Table 2. Selected Bond Lengths (Å) and Angles (deg) for 4

molecule a		molecule b	
O(10a)−Zr(1a)	1.956(3)	O(10b)−Zr(2b)	1.933(3)
O(20a)−Zr(1a)	1.930(3)	O(60b)−Zr(1b)	1.943(4)
O(60a)−Zr(2a)	1.950(3)	O(40b)−Zr(1b)	1.933(3)
O(50a)−Zr(2a)	1.955(3)	O(7b)−Zr(2b)	2.221(4)
O(30a)−Zr(1a)	2.054(3)	O(3b)−Zr(2b)	2.353(3)
O(7a)−Zr(1a)	2.174(3)	O(3b)−Zr(1b)	2.162(3)
O(3a)−Zr(1a)	2.242(3)	O(7b)−Zr(1b)	2.251(3)
O(3a)−Zr(2a)	2.195(3)	O(30b)−Zr(2b)	1.940(4)
O(7a)−Zr(2a)	2.371(3)	O(20b)−Zr(2b)	1.957(3)
O(40a)−Zr(2a)	1.935(3)	O(50b)−Zr(2b)	2.370(3)
Zr(2a)−Zr(1a)	3.2613(7)	O(50b)−Zr(1b)	2.059(4)
S(5a)−Zr(1a)	2.7401(13)	S(5b)−Zr(1b)	2.7682(14)
C(10a)−O(10a)−Zr(1a)	153.8(3)	Zr(1b)−Zr(2b)	3.2601(7)
C(20a)−O(20a)−Zr(1a)	175.7(4)	C(10b)−O(10b)−Zr(2b)	170.5(3)
C(60a)−O(60a)−Zr(2a)	156.3(4)	C(60b)−O(60b)−Zr(1b)	155.8(4)
C(50a)−O(50a)−Zr(2a)	157.9(4)	C(40b)−O(40b)−Zr(1b)	168.4(4)
C(30a)−O(30a)−Zr(1a)	130.6(3)	C(7b)−O(7b)−Zr(2b)	138.9(3)
C(7a)−O(7a)−Zr(1a)	121.7(3)	C(3b)−O(3b)−Zr(2b)	127.3(3)
C(3a)−O(3a)−Zr(1a)	125.9(3)	C(3b)−O(3b)−Zr(1b)	122.9(3)
C(3a)−O(3a)−Zr(2a)	137.6(3)	C(7b)−O(7b)−Zr(1b)	125.5(3)
C(7a)−O(7a)−Zr(2a)	128.7(3)	C(30b)−O(30b)−Zr(2b)	159.8(4)
C(40a)−O(40a)−Zr(2a)	166.3(4)	C(20b)−O(20b)−Zr(2b)	155.9(4)
S(5a)−Zr(1a)−O(30a)	140.71(10)	C(50b)−O(50b)−Zr(2b)	130.2(3)
O(10a)−Zr(1a)−O(7a)	159.10(13)	C(50b)−O(50b)−Zr(1b)	126.8(3)
O(20a)−Zr(1a)−O(3a)	170.05(14)	S(5b)−Zr(1b)−O(50b)	139.51(10)
O(40a)−Zr(2a)−O(3a)	155.33(14)	O(60b)−Zr(1b)−O(3b)	158.81(15)
O(50a)−Zr(2a)−O(7a)	158.60(14)	O(40b)−Zr(1b)−O(7b)	167.50(14)
O(60a)−Zr(2a)−O(30a)	162.30(14)	O(10b)−Zr(2b)−O(7b)	157.01(14)
O(10a)−Zr(1a)−O(20a)	97.60(15)	O(30b)−Zr(2b)−O(3b)	160.55(14)
O(50a)−Zr(2a)−O(60a)	100.57(15)	O(20b)−Zr(2b)−O(50b)	160.34(14)
O(3a)−Zr(1a)−O(7a)	73.20(12)	O(40b)−Zr(1b)−O(60(b)	98.68(16)
O(3a)−Zr(2a)−O(7a)	70.31(12)	O(20b)−Zr(2b)−O(30b)	98.59(16)
O(20a)−Zr(1a)−O(40a)	105.13(14)	O(3b)−Zr(1b)−O(7b)	73.80(12)
O(30a)−Zr(2a)−O(40a)	88.26(13)	O(3b)−Zr(2b)−O(7b)	70.75(12)

Table 3. Selected Bond Lengths (Å) and Angles (deg) for 7

S(1)−Ti(1)	3.480	C(6)−O(2)−Ti(1)	142.51(16)
O(1)−Ti(1)	1.7902(17)	O(1)−Ti(1)−O(2)	113.23(8)
O(2)−Ti(1)	1.8008(16)	C(4)−S(1)−C(5)	102.55(14)
C(5)−H(5A′)	2.963	O(1)−Ti(1)−O(1′)	110.94(14)
C(5)−H(5A)−S(1′)	169.23	O(2)−Ti(1)−O(2′)	104.02(11)
C(1)−O(1)−Ti(1)	149.96(15)	O(1)−Ti(1)−O(2′)	107.66(8)

Table 4. Selected Bond Lengths (Å) and Angles (deg) for 11 and 13

11		**13**	
O(1)−Zr(1)	1.9025(11)	O(1)−Ti(1)	1.761(2)
O(2)−Zr(1)	1.9137(12)	O(2)−Ti(1)	1.765(2)
O(3)−Zr(1)	2.3000(11)	O(3)−Ti(1)	2.2083(19)
O(4)−Zr(1)	2.3131(11)	O(4)−Ti(1)	2.2181(18)
Cl(1)−Zr(1)	2.5026(4)	Cl(1)−Ti(1)	2.3941(8)
Cl(2)−Zr(1)	2.4807(4)	Cl(2)−Ti(1)	2.3650 (8)
S(1)−Zr(1)	4.072	S(1)−Ti(1)	4.061
C(1)−O(1)−Zr(1)	161.43(11)	C(1)−O(1)−Ti(1)	160.05(19)
C(4)−O(2)−Zr(1)	154.72(11)	C(4)−O(2)−Ti(1)	154.6(2)
C(3)−S(1)−C(2)	103.23(10)	C(3)−S(1)−C(2)	103.3(2)
O(2)−Zr(1)−O(4)	170.49(5)	O(2)−Ti(1)−O(4)	168.86(9)
O(1)−Zr(1)−O(3)	170.39(5)	O(1)−Ti(1)−O(3)	169.03(8)
O(1)−Zr(1)−O(2)	100.16(5)	O(1)−Ti(1)−O(2)	101.76(9)
O(3)−Zr(1)-O(4)	81.33(4)	O(3)−Ti(1)-O(4)	79.80(7)
Cl(2)−Zr(1)-Cl(1)	160.810(15)	Cl(2)−Ti(1)-Cl(1)	163.66(3)

determined by single-crystal X-ray diffraction. Crystallographic data and selected bond distances and angles are listed in Tables 1−5. For the sake of clarity, the bis-THF adducts $MCl_2\{OSO^{Me}\}(THF)_2$ (M = Zr, **11**; M = Ti, **13**) will be discussed first.

Both **11** and **13** adopt six-coordinate, distorted octahedral, monomeric structures in the solid state (Figures 4 and 5). There is no bonding interaction between the sulfur atom and metal centers (M···S = 4.06−4.07 Å), probably due to the presence of the two THF ligands. The chloride ligands are *trans* to each other and are *cis* to the alkoxide ligand. The major distortions from idealized octahedral geometry involve the chloride ligands (Cl(1)−M(1)−Cl(2) = 160.81(2)° for **11** and 163.66(3)° for **13**). The Zr−O distances involving the dialkoxide ligand of **11** (1.902(1), 1.914(1) Å) are similar to those in the related complexes $Zr[N\{CH_2CH_2C(O)Me_2\}_2\{(S)\text{-}2\text{-}C_6H_4C(H)Me\}][CH_2Ph]$ (1.93(1), 1.938(9) Å)[4] and $Zr[PhCH_2N\{CH_2C(O)Me_2\}_2][CH_2Ph]_2$ (1.963(1), 1.967(1) Å)[7] and somewhat shorter than those in the more sterically constrained $Zr(CH_2Ph)_2$(2,6-bis{menthoxo}pyridyl) (1.989(2), 2.001(3) Å)[5] and in $Zr(CH_2Ph)_2$-$[\{-CH_2N(Me)CH_2C(CF_3)_2O\}_2]$ (2.0214(8), 2.0471(8) Å), which contains a fluorinated dialkoxide ligand.[18] The Ti−O distances in **13** are ca. 0.14 Å shorter than the corresponding Zr−O distances in **11**, reflecting the ca. 15% difference in the metal ionic radii.[19] The M−O−C units in **11** and **13** (range of M−O−C angles: 154.6−161.4°) are slightly bent, but less so than those in $Zr[N\{CH_2CH_2C(O)Me_2\}_2\{(S)\text{-}2\text{-}C_6H_4C(H)Me\}][CH_2$-

(15) (a) Eisch, J. J.; Owuor, F. A.; Shi, X. *Organometallics* **1999**, *18*, 1583−1585. (b) Eisch, J. J.; Owuor, F. A.; Otieno, P. O. *Organometallics* **2001**, *20*, 4132−4134.

(16) (a) Gothelf, K. V.; Jorgensen K. A. *J. Org. Chem.* **1994**, *59*, 5687−5691. (b) Manivannan, R.; Sundararajan, G. *Macromolecules* **2002**, *35*, 7883−7890.

(17) Mack, H.; Eisen, M. S. *J. Chem. Soc., Dalton Trans.* **1998**, 917−921.

(18) Lavanant, L.; Chou, T.-Y.; Chi, Y.; Lehmann, C. W.; Toupet, L.; Carpentier, J.-F. *Organometallics* **2004**, *23*, 5450−5458.

(19) Effective ionic radii for six-coordinate metal centers: Ti^{4+}, 0.605 Å; Zr^{4+}, 0.72 Å. Shannon, R. D. *Acta Crystallogr., Sect. A* **1976**, *A32*, 751−767.

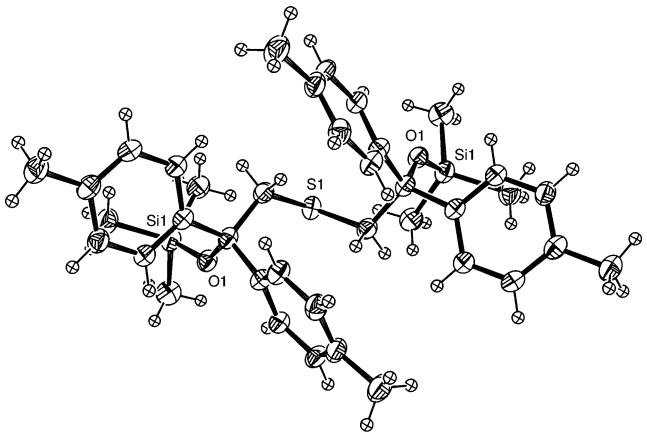

Figure 3. ORTEP drawing of $\{OSO^{tol}\}(SiMe_3)_2$ (**3b**). Ellipsoids are drawn at the 50% probability level.

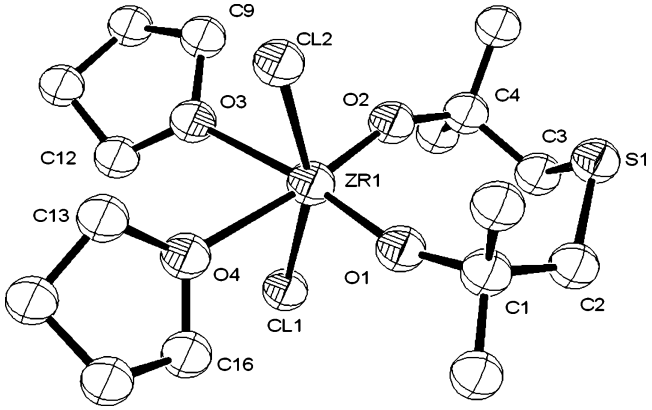

Figure 4. ORTEP drawing of $ZrCl_2\{OSOMe\}(THF)_2$ (**11**). Ellipsoids are drawn at the 50% probability level; all hydrogen atoms have been omitted for clarity.

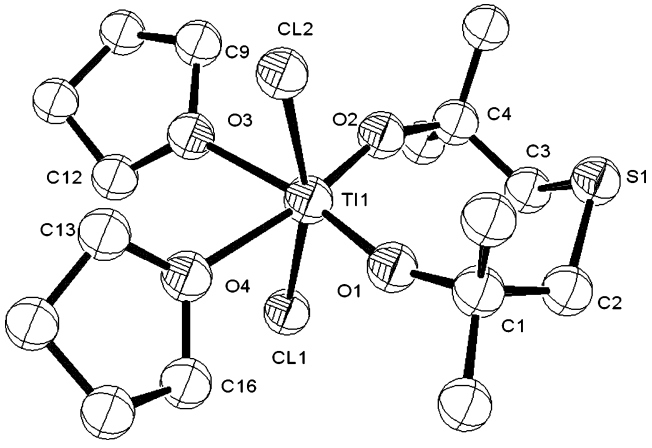

Figure 5. ORTEP drawing of $TiCl_2\{OSOMe\}(THF)_2$ (**13**). Ellipsoids are drawn at the 50% probability level; all hydrogen atoms have been omitted for clarity.

Ph] (140.4(1)°, 145.2(1)°),[4] $Zr(CH_2Ph)_2$(2,6-bis{menthoxo}pyridyl) (128.66°, 130.49°),[5] and $MX_2[\{-CH_2N(Me)CH_2C(CF_3)_2O\}_2]$ (Ti−O−C: 129.8(1)°, 129.4(1)°; Zr−O−C: 127.58(7)°, 130.75(7)°).[18] The alkoxide ligands in those species are incorporated into six- and five-membered rings, which may constrain the M−O−C angle more than flexible eight-membered rings in **11** and **13**. Overall, **11** and **13** are best described as 16-electron species (counting the alkoxides as four-electron donors).

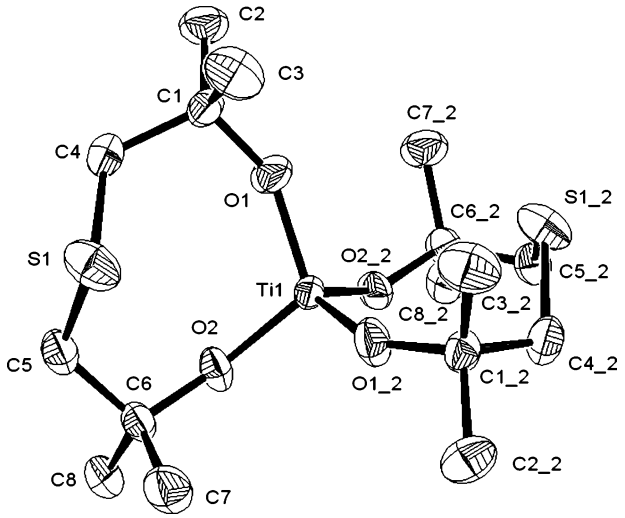

Figure 6. ORTEP drawing of $Ti\{OSOMe\}_2$ (**7**). Ellipsoids are drawn at the 50% probability level; all hydrogen atoms have been omitted for clarity.

The structure of the bis-ligand titanium complex **7** is shown in Figure 6. The Ti center has a slightly distorted tetrahedral coordination geometry, with only the O atoms bound to the metal center (range of O−Ti−O angles = 104.0(1)−113.23(8)°). The Ti−O distances are similar to those in **13**, while the Ti−O−C angles are ca. 10° smaller (149.9(1)° and 142.5(2)°). The S atom in **7** is not coordinated (Ti···S = 3.480 Å). This contrasts with the structure of the six-coordinate bis(aminodialkoxide) complex $Zr[MeN\{CH_2CH_2C(O)Ph_2\}_2]_2$, in which both N atoms are coordinated to the metal center.[20] This may not be surprising since (i) Zr normally prefers a higher coordination number vs Ti and (ii) the hard metal ion (Ti, Zr) is expected to prefer dative interactions with relatively harder nitrogen atoms than soft sulfur atoms.[21,22]

However, as shown in Figure 7, the S atoms are involved in intermolecular S···H···C interactions with methylene groups adjacent to sulfur in neighboring molecules, which results in a linear chain packing arrangement. The S···H distance of 2.96 Å is close to the sum of the S and H van der Waals radii (3.00 Å) and is similar to the distances observed for intermolecular C−H···S interactions in tetrathiafulvalene derivatives.[23]

The crystal structure of the heteroleptic complex $Zr(OtBu)_2\{OSO^{Me}\}$ (**4**) is more complicated than those of **11**, **13**, and **7**. It features two independent dinuclear molecules that differ in the nature of the bridging

(20) Shao, P.; Gendron, R. A. L.; Berg, D. J. *Can. J. Chem.* **2000**, *78*, 255−264.

(21) Note that $-CPh_2O^-$ is a poorer donor as compared to $-CMe_2O^-$, which is anticipated to facilitate N coordination.

(22) Note that a Zr···S bonding interaction with a distance of 2.7657(8) Å has been established in the bis(sulfur-bridged binaphtholate) zirconium complex $Zr[1,1'\text{-}S(2\text{-}OC_{10}H_4\text{-}t\text{Bu}_2\text{-}3,6)_2]_2$(THF), despite the presence of an additional coordinated THF molecule and a much more severe constraint within the five-membered Zr−O−aryl−S rings; see ref 9e.

(23) (a) Jung, D.; Evain, M.; Novoa, J. J.; Whangbo, M.-H.; Beno, M. A.; Kini, A. M.; Schultz, A. J.; Williams, J. M.; Nigrey, P. J. *Inorg. Chem.* **1989**, *28*, 4516−4522. (b) Rovira, C.; Novoa, J. *Chem. Phys. Lett.* **1997**, *279*, 140−150, and references therein.

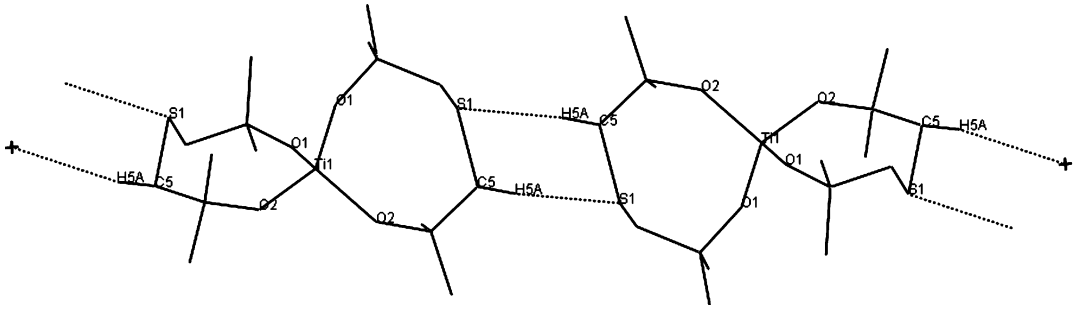

Figure 7. Intermolecular S···H interactions in Ti{OSOMe}$_2$ (**7**). All hydrogen atoms except those involved in the interactions have been omitted for clarity.

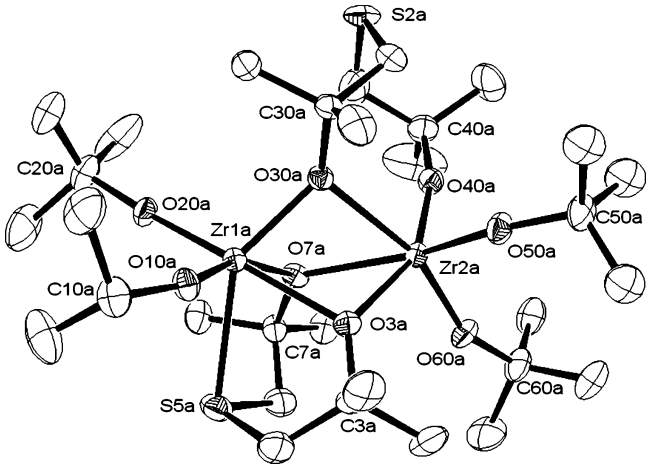

Figure 8. ORTEP drawing of the molecule a of complex **4**. Ellipsoids are drawn at the 50% probability level; all hydrogen atoms have been omitted for clarity.

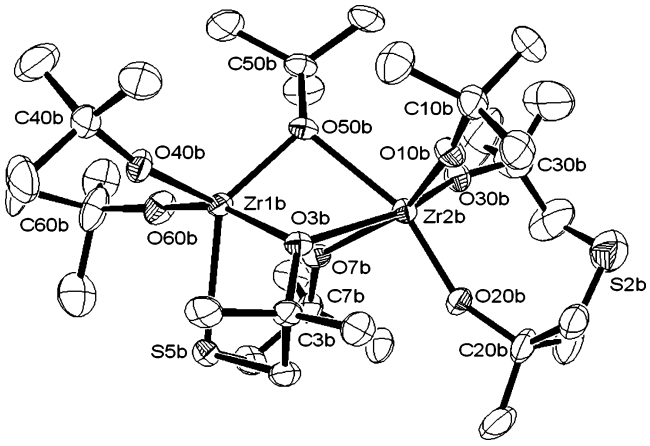

Figure 9. ORTEP drawing of the molecule b of complex **4**. Ellipsoids are drawn at the 50% probability level; all hydrogen atoms have been omitted for clarity.

ligands (**4a**, Figure 8; **4b**, Figure 9). In **4a**, two Zr(O*t*Bu)$_2$units are linked by a μ,μ-OSO^{Me} ligand (O7a−O3a), which bridges Zr1a and Zr2a by both oxygens and is also S-bonded to Zr1a, and by a μ-OSO^{Me} ligand (O30a−O40a), which bridges Zr1a and Zr2a by one oxygen and is terminal to Zr2a through the other. Molecule **4b** differs from **4a** by exchange of the bridging arm of the μ-OSO^{Me} ligand by a O*t*Bu ligand. The coordination environment at Zr(1) is thus similar in both molecules and is best described as strongly distorted octahedral. Also, the second Zr atom (Zr(2)) is coordinated by six oxygen atoms in a strongly distorted octahedral environment in both **4a** and **4b**. The Zr−O distances (1.935(3)−1.957(3) Å) involving nonbridging oxygen atoms of the dialkoxide ligand are somewhat longer than those found in **11** and unexceptional (2.054(3)−2.371(3) Å) for those involving bridging oxygen atoms.[9e,24] The Zr−S distances (**4a**, 2.7401(13); **4b**, 2.768(1) Å) are similar to that (2.7657(8) Å) in the sulfur-bridged binaphtholate zirconium complex Zr[1,1′-S(2-OC$_{10}$H$_4$-*t*Bu$_2$-3,6)$_2$]$_2$(THF).[9e]

Solution Structure and Dynamics of Neutral Complexes. The solution structures of **8**, **12**, and **4** have been investigated in detail by NMR techniques.[25] NMR studies were performed in toluene or benzene solvents to avoid the formation of solvent adducts.

The low-temperature (230 K) ^{1}H NMR spectrum of Zr(CH$_2$Ph)$_2${OSO^{Me}} (**8**) in toluene-d_8 features sharp signals (Figure 10). Key resonances include two singlets for the ZrC*HH*Ph groups, two AB doublets for the SC*HH* groups, and two (partially overlapping) singlets for the C*Me*$_2$ groups. The 220 K ^{13}C NMR spectrum of **8** contains two sets of benzyl resonances, one SCH$_2$ resonance, and two methyl resonances. These data are consistent with overall C_s symmetry. The observation of two benzylic *C*H$_2$ ^{13}C signals with well-differentiated J_{C-H} coupling constants (δ 54.9, J_{C-H} = 139.3 Hz; δ 53.6, J_{C-H} = 128.5 Hz) and two C$_{ipso}$ signals, with one at high-field (δ 147.6 and 136.5), is diagnostic for the presence of one η^2-benzyl group and one normal η^1-benzyl group.[5,26] Coordination of the S atom to Zr in **8** is likely, but the NMR data give no definitive evidence for it.[27]

As shown in Figure 10, raising the temperature results in broadening and coalescence of the ZrC*H*$_2$Ph

(24) (a) Heyn, R. H.; Stephan, D. W. *Inorg. Chem.* **1995**, *34*, 2804−2812. (b) Boyle, T. J.; Schwartz, R. W.; Doedens, R. J.; Ziller, J. W. *Inorg. Chem.* **1995**, *34*, 1110−1120. (c) Swamy, K. C. K.; Veith, M.; Huch, V.; Mathur, S. *Inorg. Chem.* **2003**, *42*, 5837−5843. (d) Evans, W. J.; Ansari, M. A.; Ziller, J. W. *Polyhedron* **1998**, *17*, 869−878.

(25) The NMR spectra of the six-coordinated bis(THF) complexes **11** and **13** are consistent with the structures observed in the solid state. The solution structure and dynamics of **9** could not be investigated in a noncoordinating solvent, since this complex is only soluble in THF (suggesting it exists as strongly agglomerated species in noncoordinating solvents).

(26) (a) Latesky, S. L.; McMullen, A. K.; Nicollai, G. P.; Rothwell, I. P. *Organometallics* **1985**, *4*, 902−908. (b) Jordan, R. F.; Lapointe, R. E.; Bajgur, C. S.; Echols, S. F.; Willett, R. *J. Am. Chem. Soc.* **1987**, *109*, 4111−4113. (c) Bochmann, M.; Lancaster, S. J.; Hursthouse, M. B.; Abdul Malik, K. M. *Organometallics* **1994**, *13*, 2235−2243.

(27) No clear trend was observed in the ^{1}H and ^{13}C chemical shifts of SC*H*$_2$ units in complexes prepared in this study that could be related to coordination of S to the metal center. However, coordination of N to Zr has been observed in the solid-state structure of the parent complex Zr(CH$_2$Ph)$_2${ONO^{Me}}; see ref 7.

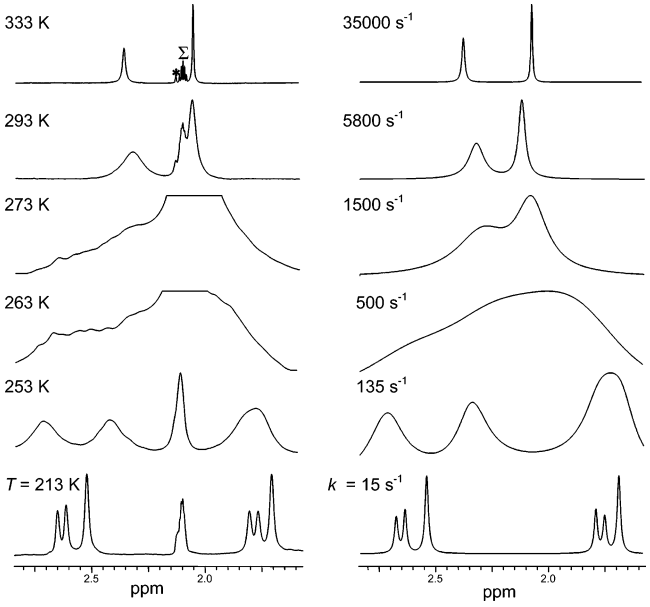

Figure 10. Experimental (left) and simulated (right) variable-temperature ^{1}H NMR spectra of $Zr(CH_2Ph)_2\{OSO^{Me}\}$ (**8**) (toluene-d_8, 300 MHz) showing the ZrCH_2Ph (δ 1.40 and 2.55) and SCH_2 (δ 1.55 and 2.75) resonances. The vertical expansion is different in each case for clarity. Best-fit first-order rate constants (k) are shown with the simulated spectra (* and Σ denote resonances for PhCH_3 and PhCHD_2, respectively).

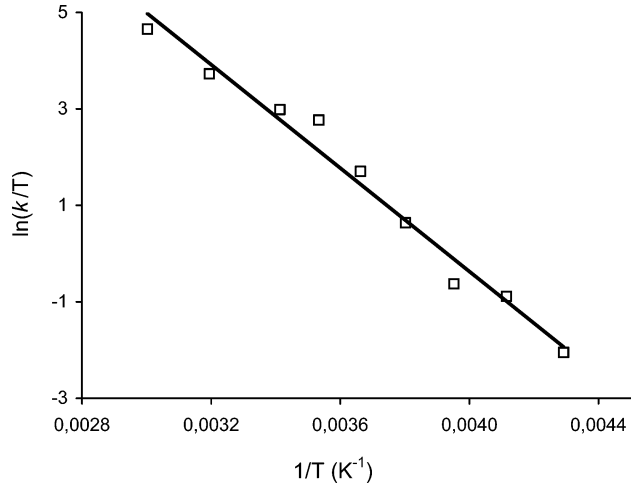

Figure 11. Eyring plot for $Zr(CH_2Ph)_2\{OSO^{Me}\}$ (**8**) (toluene-d_8 solvent) ($R^2 = 0.977$).

resonances and of the SCH_2 resonances, and at 333 K sharp singlets are observed for those groups. A single set of resonances for equivalent SCH_2, CMe_2, and benzylic groups is also observed in the room-temperature ^{13}C NMR spectrum of **8**. These data establish that **8** undergoes exchange of the η^2/η^1-benzyl ligands, as shown in eq 6.[5] Line-shape analysis demonstrated that both the ZrCH_2Ph hydrogens and the SCH_2 hydrogens exchange at the same (or at least quite similar) rates (Figure 10), as expected for the fluxional process in eq 6.[28] The activation parameters for this fluxional behavior ($\Delta H^‡ = 10.6 \pm 1$ kcal·mol^{-1}; $\Delta S^‡ = -2.7 \pm 2$ cal·mol^{-1}·K^{-1}) were derived from an Eyring analysis (Figure 11).[29] The activation parameters for **8** differ from those for benzyl exchange in $Zr(CH_2Ph)_2\{ONO^{Me}\}$ ($\Delta H^‡ = 20.0 \pm 1$ kcal·mol^{-1}; $\Delta S^‡ = 13.1 \pm 2$ cal·mol^{-1}·K^{-1}),[21] which occurs unambiguously via a dissociative mechanism.[7,30]

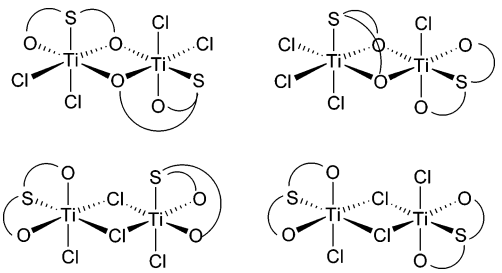

Figure 12. Plausible C_1-symmetric dimeric structures for $TiCl_2\{OSOMe\}$ (**12**).

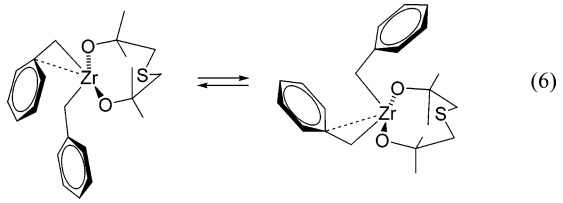

(6)

The room-temperature ^{1}H NMR spectrum of $TiCl_2\{OSO^{Me}\}$ (**12**) in toluene-d_8 consists of only two sharp singlets for the CMe_2 and SCH_2 groups. Upon lowering the temperature, these resonances broaden and split and, at 218 K, one major series of resonances is present (accounting for ca. 90% of the product), which comprises eight doublets for the SCHH groups and eight singlets for the CH_3 groups. Also, four SCH_2CMe_2O groups were distinguished by 2D NMR experiments (HMBC, HMQC, and COSY) and each group integrated equally. From these NMR data, and the X-ray structures of related sulfur-bridged bis(phenoxide) titanium complexes,[10c,12a] we propose that **12** exists in toluene solution as a single C_1-symmetric dimer. Dimerization of **12** is plausible since stabilization of the electron-deficient metal center cannot proceed intramolecularly as in benzyl complex **8**. The observation of two low-field (δ 96.1 and 96.0) and two high-field (δ 92.6 and 91.1) $C-$O resonances in the ^{13}C NMR spectrum of **12** suggests that dimerization of **12** occurs by double bridging from the oxygen atoms of the dialkoxide ligand[10c] rather than μ-Cl bridging[12a] (Figure 12).

Similarly, the room-temperature ^{1}H NMR spectrum of $Zr(OtBu)_2\{OSO^{Me}\}$ (**4**) consists of sharp singlets for the CMe_2, SCH_2 groups, and *tert*-butoxide groups of appropriate relative intensity. The 233 K ^{1}H spectrum is quite complicated, contains three series of resonances (accounting for >90% of the product) of comparable intensity. Most of the CMe_2 and O*t*Bu resonances

(28) Simulation of the OCMe_2 resonances was not attempted because of the minute difference in the chemical shifts.

(29) (a) These values correspond well with the free energy of activation determined experimentally from the coalescence temperature (T_c = ca. 270 K) for both the ZrCH_2Ph and SCH_2 hydrogens ($\Delta G_{coal}^‡ = 11.3(3)$ kcal·mol^{-1}, $\Delta G_{calc}^‡ = 11.3$ kcal·mol^{-1}). Exchange barriers $\Delta G^‡$ were determined from the coalesence of the SCHH AB patterns using the following equations for an equally populated, two-site exchange: $\Delta G^‡ = 4.576T_c[10.319 + \log(T_c/k_c)]$, where T_c is the coalesence temperature and k_c is the exchange rate constant at coalesence, which is given by $k_c = \pi[(\Delta\nu_{AB}^2 + 6J_{AB}^2]^{1/2}/2^{1/2}$.[b-d] The errors on $\Delta G_{coal}^‡$ were estimated assuming ±2% uncertainty in the chemical shifts and coalescence temperature. (b) Alexander, S. *J. Chem. Phys.* **1962**, *37*, 967−974. (c) Kurland, R. J.; Rubin, M. B.; Wise, W. B. *J. Chem. Phys.* **1964**, *40*, 2426−2427. (d) Kost, D.; Zeichner, A. *Tetrahedron Lett.* **1974**, 4533−4536.

overlap at 233 K, which hampers valuable analysis. In contrast, the SC*HH* hydrogens were well resolved. Two of the three series of resonances are composed of eight doublets for the SC*HH* groups, while the third series contains only four doublets for the SC*HH* groups. In the 233 K HMQC spectrum, the three series of hydrogens correlate respectively with two series of four SCH_2 carbons and one series of two SCH_2 carbons. It is reasonable to assume that the first two series of resonances can be assigned to the dimeric C_1-symmetric molecules **4a** and **4b** observed in the solid-state structure of **4**, which differ in the nature of the μ-bridging ligands. The third series may correspond to a C_2/C_s-symmetric dimer or a C_1-symmetric mononuclear species.

Although the nuclearity of all $[MX_2\{OSO^{Me}\}]_n$ species could not be unambiguously established, mononuclear and dinuclear structures appear as the most plausible hypotheses. For both **4** and **12**, fast symmetrization of the putative dinuclear structures on the NMR time scale occurs at high temperature. This is likely to proceed via intramolecular ligand exchange, and there is no evidence for the formation of mononuclear species in apolar solvents. It seems therefore that the nuclearity of electron-deficient $MX_2\{OSO^{Me}\}$ species is controlled by the nature of the X ligands (X = CH_2Ph, Cl, OR). Among those investigated in this work, only the benzyl ligands enable stabilizing mononuclear species in solution, possibly thanks to their intramolecular η^2-coordination mode, while chloro and alkoxide ligands induce bridging modes and formation of dinuclear species.

Generation of Cationic Benzyl-Zirconium Complexes. The reaction of $Zr(CH_2Ph)_2\{OSO^{Me}\}$ (**8**) with $[Ph_3C][B(C_6F_5)_4]$[31] at 240 K resulted in the almost instantaneous formation of 1 equiv of Ph_3CCH_2Ph[32] and a yellow-orange complex characterized by ^1H, ^{11}B, ^{13}C, and ^{19}F NMR spectroscopy as the cationic complex $[Zr(CH_2Ph)\{OSO^{Me}\}][B(C_6F_5)_4]$ (**15**, eq 6). Complex **15** separates from toluene solution as an orange oil, which is soluble and relatively stable at 240 K in CD_2Cl_2 solution (in the absence of excess trityl reagent). Significant decomposition of **15** and/or reaction with the solvent to produce mixtures of unidentified products was observed, however, after 2 h at 240 K in CD_2Cl_2 and was complete within 20 min at room temperature.

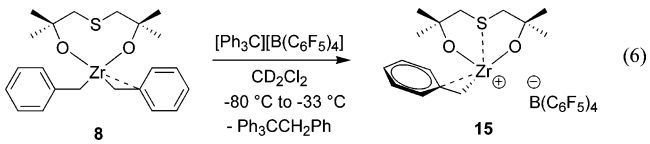

(6)

As expected, no evidence was found for coordination of the $[B(C_6F_5)_4]^-$ counteranion in **15**: ^{19}F NMR resonances were unperturbed from the free anion values. The ^1H and ^{13}C NMR spectra show that **15** has a nonfluxional C_1-symmetric structure up to 273 K, at which temperature fast decomposition proceeds. The ^1H NMR spectrum of **15** (240 K) contains four singlets for the Me groups, four doublets for the SC*HH* groups, and two doublets for the PhC*HH* hydrogens (Figure 13). A complete set of ^{13}C resonances is observed, which are particularly well differentiated for the methylene groups adjacent to the sulfur atom (δ 59.9 and 51.3). The Zr-benzyl *ipso*-carbon ^{13}C resonance appears at high-field (δ 132.4, assigned by the HMBC correlation with PhC*HH*), consistent with η^2-benzyl coordination,[26] as in the parent neutral complex **8**. Also, the ^1H NMR spectrum of **15** exhibits a 1:2:2 pattern of downfield resonances (δ 8.30, *p*-H; 7.91, *m*-H; 7.69, *o*-H) for the benzyl group that indicates a very strong interaction of the phenyl ring with the metal center.[34] Additionally, complex **15** may be further stabilized by solvent coordination.

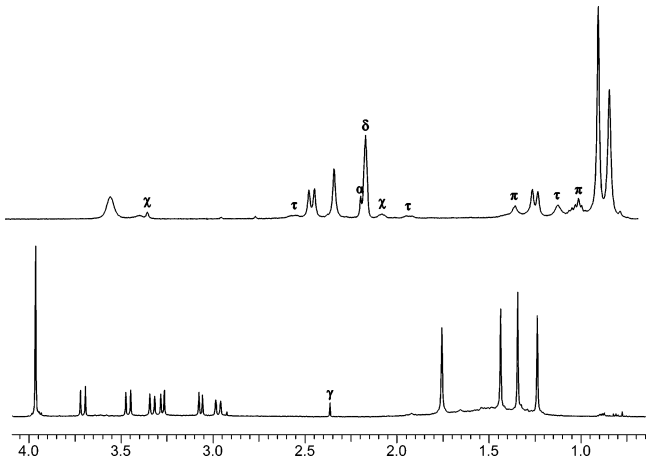

Figure 13. ^1H NMR spectra (400 MHz, 240 K) of $[Zr(CH_2Ph)\{OSO^{Me}\}][B(C_6F_5)_4]$ (**15**) (CD_2Cl_2, bottom) and $[Zr(CH_2Ph)\{OSO^{Me}\}][B(CH_2Ph)(C_6F_5)_3]$ (**16**) (toluene-d_8, top). The markers α, δ, and γ denote resonances for $PhCH_3$, $PhCHD_2$, and $CHDCl_2$, respectively; the marker τ denotes the resonances for the neutral complex $Zr(CH_2Ph)_2\{OSO^{Me}\}$ (**8**); the markers π and χ denote resonances for pentane and organic impurities, respectively.

Generation of $Zr(CH_2Ph)\{OSO^{Me}\}^+$ species by reaction of **8** with $B(C_6F_5)_3$ was also investigated.[31f,33] Addition of cold toluene to a mixture of **8** and $B(C_6F_5)_3$ at 243 K resulted in the virtually instantaneous generation of an intense yellow color, indicating rapid alkyl abstraction. The product exhibited high solubility in toluene and has been characterized by ^1H, ^{11}B, ^{13}C, and ^{19}F NMR spectroscopy as the zwitterion $Zr(CH_2Ph)\{OSO^{Me}\}^+(\mu\text{-}\eta^6,\eta^1\text{-}PhCH_2B(C_6F_5)_3]^-$ (**16**, eq 7). Anion coordination to zirconium via a η^6 π-benzene interaction was clearly indicated by the characteristic downfield location of the

(30) Purely dissociative mechanisms are generally characterized by $\Delta S^{\ddagger}$ values above 10 eu. See: (a) Atwood, J. D. *Inorganic and Organometallic Reaction Mechanisms*; Brooks/Cole: Monterey, CA, 1985; p 17. (b) Jordan, R. B. *Reaction Mechanisms of Inorganic and Organometallic Systems*; Oxford University: New York, 1991; pp 56−57.

(31) For use of $[Ph_3C][B(C_6F_5)_4]$ in the generation of $L_nM(R)^+$ species, see: (a) Chien, J. C. W.; Tsai, W.; Rausch, M. D. *J. Am. Chem. Soc.* **1991**, *113*, 8570−8571. (b) Ewen, J. A.; Elder, M. J. *Makromol. Chem., Macromol. Symp.* **1993**, *66*, 179−190. (c) Bochmann, M.; Lancaster, S. *Organometallics* **1993**, *12*, 633−640. (d) Razavi, A.; Thewalt, U. *J. Organomet. Chem.* **1993**, *445*, 111−114. (e) Straus, D. A.; Zhang, C.; Tilley, T. D. *J. Organomet. Chem.* **1989**, *369*, C13−C17. (f) Chen, E. Y.-X.; Marks, T. J. *Chem. Rev.* **2000**, *100*, 1391−1434.

(32) Stoebenau, E. J.; Jordan, R. F. *J. Am. Chem. Soc.* **2003**, *125*, 3222−3223.

(33) For use of $B(C_6F_5)_3$ in the generation of $M(R)L_n^+$ species, see: (a) Jordan, R. F. *Adv. Organomet. Chem.* **1991**, *32*, 325−387. (b) Yang, X.; Stern, C. L.; Marks, T. J. *J. Am. Chem. Soc.* **1994**, *116*, 10015−10031, and references therein.

(34) Horton, A. D.; de With, J. *Organometallics* **1997**, *16*, 5424−5436.

B-benzyl *ipso*-C ^{13}C NMR resonance at δ 159.2 in **16** (compared to δ 148.5 for the free anion),[34,35] downfield shift of the *meta*- and *para*-fluorine ^{19}F resonances relative to those of the free anion, and the difference in the chemical shifts of the *meta*- and *para*-fluorine ^{19}F resonances ($\Delta\delta(m,p\text{-F}) = 3.7$).[34] The high solubility of **16** in toluene solution is also consistent with benzylborate anion coordination to the metal center, rather than a solvent-separated ionic structure. The ^{1}H NMR spectrum of **16** in the temperature range 230−250 K contains two singlets for the methyl groups, two doublets for the SC*HH* hydrogens, and a broadened singlet for the Zr-C*HH*Ph hydrogens, consistent with a C_s-symmetric structure.[36]

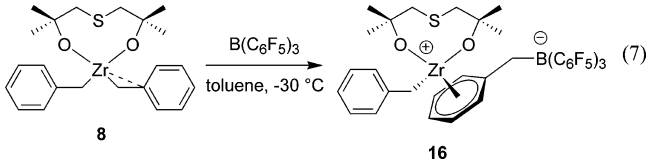

(7)

However, despite the anion coordination, **16** is thermally sensitive and converts cleanly to a second species (**17**) over several hours at 296 K and much faster at higher temperatures. The conversion was monitored by ^{1}H, ^{11}B, ^{13}C, and ^{19}F NMR spectroscopy. ^{11}B NMR monitoring (see Supporting Information) indicated that **16** (δ −11.4) is selectively transformed into another *ionic* species, **17**, which also has a four-coordinate anionic boron center slightly shifted upfield (δ −11.7). The ^{19}F NMR spectrum of **17** contains three *ortho*-fluorine resonances: two at δ −114.9 and −128.2 that integrate respectively for 1 *o*-F and are characteristic of a C_6F_5 group (unsymmetrically) coordinated onto Zr,[37,39] and a third one at δ −130.5 for 4 *o*-F of a $(PhCH_2)_2B(C_6F_5)_2^-$ group.[38] In the aromatic region of the ^{1}H NMR spectrum (Figure 14), in addition to a normal pattern of resonances for a typical benzyl group, three separate resonances were observed for the phenyl hydrogens of the other benzyl moiety. The upfield shift of some of these resonances from their usual positions is indicative of coordination of the phenyl ring to the metal center.[38] Similar features were evident in the ^{13}C{^{1}H} NMR spectrum. Also, the ^{1}H and ^{13}C{^{1}H} NMR spectra contain respectively two singlets at δ 3.45 and 2.88, and two broad resonances at δ 38.2 and 35.2 for the two BCH_2 groups, consistent with previous assignments on closely related species.[38] Moreover, no resonances attributable to a Zr-CH_2Ph moiety were observed in the ^{1}H and ^{13}C NMR spectra of **17**. On the basis of these data, corroborated by 2D HMQC, HMBC, and COSY

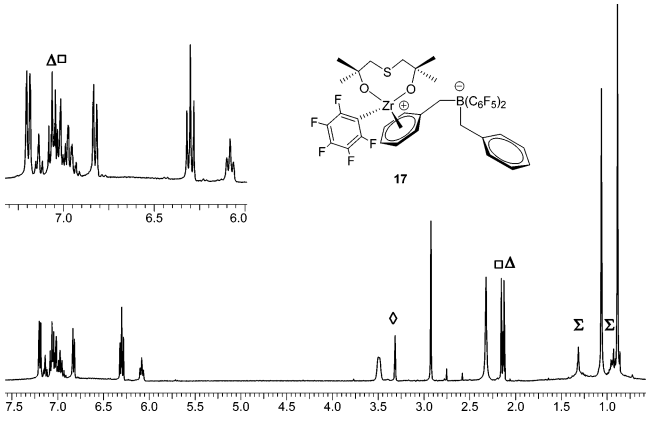

Figure 14. ^{1}H NMR spectrum (toluene-d_8, 400 MHz, 296 K) of the decomposition product from **16** ($[Zr(C_6F_5)\{OSOMe\}]^+[\eta^6\text{-}(PhCH_2)B(CH_2Ph)(C_6F_5)_2]^-$, **17**). The markers △ and □ denote resonances for PhCH_3 and PhCHD_2, respectively; the markers Σ and ◇ denote resonances for pentane and unidentified impurities, respectively.

experiments, product **17** has been formulated as $[Zr(C_6F_5)\{OSO^{Me}\}]^+[\eta^6\text{-}(PhCH_2)B(CH_2Ph)(C_6F_5)_2]^-$ (eq 8).

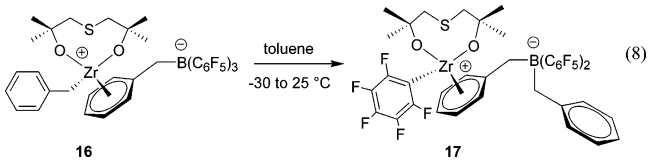

(8)

Room-temperature ^{1}H NMR data indicate an overall C_s-symmetry for **17** on the NMR time scale. As judged by ^{1}H NMR spectroscopy, complex **17** does not exhibit fluxionality in toluene in the temperature range 243−303 K. This was unexpected considering the possible exchange process between the coordinated arene and the phenyl ring of the other benzyl ring.[38] Reasons for this stability are not clear at the moment. Decomposition pathways of zirconium cationic species associated with the alkylborate $[RB(C_6F_5)_3]^-$ anion usually involve transfer of C_6F_5 fragments from boron to the metal center, to end up with *neutral* zirconium species.[5,34,39] The selective transformation of **16** to **17** suggests that the cationic center of **17** is not electrophilic enough, for electronic and/or steric reasons, to pull off a $C_6F_5^-$ substituent of the coordinated borate anions and generate in turn a neutral bis(pentafluorophenyl)zirconium complex.

Ethylene Polymerization. The prepared complexes were briefly investigated in ethylene polymerization. Neutral $MCl_2\{OSO^R\}(THF)_n$ complexes **9**−**14** were activated with MAO or a combination of $[Ph_3C][B(C_6F_5)_4]$ with Al(iBu)$_3$,[40] while molecular Lewis acidic activators were used to generate the cationic benzyl-zirconium species **15** and **16** from **8** in situ. The results are summarized in Table 5.

(35) (a) Pellecchia, C.; Grassi, A.; Immirzi, A. *J. Am. Chem. Soc.* **1993**, *115*, 1160−1162. (b) Pellecchia, C.; Immirzi, A.; Grassi, A.; Zambelli, A. *Organometallics* **1993**, *12*, 4473−4478. (c) Pellecchia, C., Grassi, A.; Zambelli, A. *J. Mol. Catal.* **1993**, *82*, 57−65.

(36) The SC*HH* and Zr-C*HH*Ph resonances broaden on raising the temperature, and coalescence of the methyl singlets is observed at 250 K, yielding a sharp singlet at room temperature. However, due to rapid decomposition above 250 K, the fluxional behavior of **16** could not be investigated in detail.

(37) (a) Bochmann, M.; Sarsfield, M. J. *Organometallics* **1998**, *17*, 5908−5912. (b) Indado, G. J.; Lancaster, S. J.; Thornton-Pett, M.; Bochmann, M. *J. Am. Chem. Soc.* **1998**, *120*, 6816−6817. (c) Kraft, B. M.; Jones, W. D. *J. Organomet. Chem.* **2002**, *658*, 132−140. (d) Stoebenau, E. J.; Jordan, R. F. *J. Am. Chem. Soc.* **2004**, *126*, 11170−11171.

(38) Spence, R. E. v. H.; Piers, W. E. *Organometallics* **1995**, *14*, 4617−4624.

(39) Gauvin, R.; Mazet, C.; Kress, J. *J. Organomet. Chem.* **2002**, *658*, 1−8, and references therein.

(40) (a) Chien, J. C. W.; Xu, B. *Makromol. Chem. Rapid Commun.* **1993**, *14*, 109−114. (b) Chien, J. C. W.; Tsai, W. M. *Makromol. Chem. Macromol. Symp.* **1993**, *66*, 141−155. (c) Chen, Y. X.; Rausch, M. D.; Chien, J. C. W. *Organometallics* **1994**, *13*, 748−749. (d) Chien, J. C. W.; Rausch, M. D. *J. Polym. Sci. Part A: Polym. Chem.* **1994**, *32*, 2387−2393. (e) Song, F. S.; Cannon, R. D.; Lancaster, S. J.; Bochmann, M. *J. Mol. Catal. A* **2004**, *218*, 21−28.

Table 5. Ethylene Polymerization Data[a]

entry	catalyst precursor	activator (equiv)	temp (°C)	time (min)	yield (g)	activity[b] (kg PE·mol^{-1}·h^{-1})	M_w[c] (10^{-3})	M_w/M_n[c]	T_m[d] (°C)
1	$TiCl_2\{OSO^{Me}\}$ (**12**)	MAO (500)	25	40	1.382	14	513	110	137.3
2	$TiCl_2\{OSO^{Me}\}$ (**12**)	MAO (500)	60	30	0.803	10	274	52	137.7
3	$TiCl_2\{OSO^{Me}\}$ (**12**)	$[Ph_3C][B(C_6F_5)_4]$ (3)/ $Al(iBu)_3$ (10)	25	30	0.152	7	138	13.6	136.7
4	$TiCl_2\{OSO^{Me}\}(THF)_2$ (**13**)	MAO (500)	25	30	0.040	1	419	14.4	135.7
5[e]	$TiCl_2\{OSO^{tol}\}$ (**14**)	MAO (700)	25	65	0.520	10	nd	nd	135.1
6	$ZrCl_2\{OSO^{Me}\}$ (**9**)	MAO (500)	25	0.08	0.041	470	nd	nd	138.6
7	$ZrCl_2\{OSO^{Me}\}$ (**9**)	MAO (500)	35	0.08	0.295	7190	1110	10.8	136.1
8	$ZrCl_2\{OSO^{Me}\}$ (**9**)	$[Ph_3C][B(C_6F_5)_4]$ (3)/ $Al(iBu)_3$ (10)	25	0.08	0.120	1130	480	2.5	141.9
9	$ZrCl_2\{OSO^{Me}\}(THF)$ (**10**)	MAO (500)	25	0.08	0.040	590	nd	nd	138.1
10[f]	$Zr(CH_2Ph)_2\{OSO^{Me}\}$ (**8**)	$B(C_6F_5)_3$ (1)	25	0.08	0.075	146	458	4.8	141.5
11[f,g]	$Zr(CH_2Ph)_2\{OSO^{Me}\}$ (**8**)	$[Ph_3C][B(C_6F_5)_4]$ (1)	25	30	0	0			

[a] Polymerization experiments were conducted under 5 atm of ethylene using 30−140 μmol of catalyst precursor in 30−80 mL of toluene; the results shown for each entry are representative of at least two reproducible runs. [b] Average activity calculated over the whole polymerization time. [c] Determined by GPC. [d] Determined by DSC. [e] Conducted under 1 atm of ethylene. [f] Conducted in the presence of 100 equiv of $Al(iBu)_3$ as scavenger. [g] No activity was observed in the absence of $Al(iBu)_3$.

Titanium complexes **12**−**14** activated by MAO in toluene solution are poorly active for ethylene polymerization (entries 1−5).[41] No discoloration of the pale orange-yellow reaction mixture was observed over 60 min and ethylene consumption continued over this period,[42] suggesting that the active species are quite stable under these conditions. However, the high molecular weights of the PEs recovered indicate poor initiation efficiencies. Increase of the temperature to 60 °C had a minor impact on the results (entries 1 and 2).

In contrast, catalysts based on zirconium complexes **9** and **10** are much more active but deactivate very fast. Under the conditions investigated (entries 6−10), all of the polyethylene is formed within 5 s, and no more ethylene is consumed after this time. The activity is significantly enhanced up to 7 tons PE·mol^{-1}·h^{-1}by raising the polymerization temperature to 35 °C instead of 25 °C (entries 6 and 7). The apparent activity is higher than those reported for related catalysts based on discrete zirconium precursors having amino-alkoxide or amino-dialkoxide ligands,[43] although direct comparisons are difficult due to differences in polymerization time and conditions. The activity observed from THF-free precursor **9** (entry 6) is comparable to that for the bis-THF complex **10** (entry 9), most likely because excess MAO traps THF. On the other hand, low or no activity was observed with discrete in situ-generated ionic complex **16** (entries 10, 11). Berg[4] and Kress[5] observed similar insignificant or no ethylene polymerization activity with $Zr(CH_2Ph)_2[RN\{CH_2CH_2C(O)R'_2\}_2]$/$B(C_6F_5)_3$ and $Zr(CH_2Ph)_2$(2,6-bis{menthoxo}pyridyl)/$B(C_6F_5)_3$ combinations, respectively, and attributed it to the formation of tight ion pairs.

The polymers produced under these conditions have a quite high molecular weight and melting temperatures in the range 135−141 °C, indicative of essentially linear long chain microstructures. The molecular weight distributions were generally broad,[43] especially for Ti systems, although most of them feature monomodal shapes with long tailing on low[42] and high molecular weights (see Supporting Information). The polyethylene produced with the **9**/$[Ph_3C][B(C_6F_5)_4]$/$Al(iBu)_3$ (1:3:10) activating combination (entry 8) had a relatively narrow monomodal molecular weight distribution, characteristic of a single-site catalyst.

Conclusions

The aim of this study was to investigate the coordination properties of the tridentate ligand systems $\{OCR_2CH_2SCH_2CR_2O\}^{2-}$ in simple neutral group 4 $MX_2\{OSO^R\}$ complexes and cationic $M(R)\{OSO^R\}^+$ alkyl species. Effective routes for the preparation of a variety of chloro, isopropoxo, amido, and benzyl Zr and Ti complexes, as well as bis-ligand complexes, have been identified with the methyl-substituted ligand system. Those compounds have been characterized in the solid state and in solution. Difficulties have been encountered in the synthesis of complexes derived from the ligand system having *p*-tolyl substituents; further studies are required to evaluate the relative influence of steric and electronic factors in this case. Remarkably, most of the $MX_2\{OSO^{Me}\}$ complexes studied adopt mononuclear structures in the solid state and in solution, despite the modest steric crowding and electron-donating capability of the ligand. Discrete cationic species $[Zr(CH_2Ph)\{OSO^{Me}\}]^+$ have also been prepared and found to be moderately stable. Although plausible, the interaction of the sulfur atom with metal centers in $MX_2\{OSO^R\}$ and $M(R)\{OSO^R\}^+$ species could not be established unambiguously.

The high ethylene polymerization activity observed with some $ZrCl_2\{OSO^R\}$/MAO combinations is in line with predictive computations carried out several years ago,[11] which forecasted the promising catalytic performances of sulfur-bridged dialkoxide complexes. However, reasons for the high activity but also high instability of these catalytic systems are still unclear. Current investigations are directed toward understanding these

(41) Eisen and co-workers have reported that the $TiCl_2[Py\{CPh_2O\}_2]$/MAO combination exhibits modest ethylene polymerization activity (20 °C, 1 atm); see ref 6b.

(42) In these experiments, polyethylene was recovered in virtually the same amount as that of ethylene consumed; oligomers (if any) are therefore negligible.

(43) (a) $Zr(CH_2Ph)_2[RN\{CH_2CH_2C(O)R'_2\}_2]$/MAO (1:500) gave at 50 °C, 5 atm 136−384 kg PE·mol^{-1}·h^{-1} with M_w = 143−452 000, M_w/M_n = 3.4−5.7; see ref 4. (b) $Zr(CH_2Ph)_2\{PyC(CF_3)_2O\}_2$/MAO (1:1000) gave at 30 °C, 8 atm 10 kg PE·mol^{-1}·h^{-1} with M_w = 375 000, M_w/M_n = 28; $Zr(CH_2Ph)_2\{PyC(CF_3)_2O\}_2/B(C_6F_5)_3$ (1:1) gave at 40 °C, 3 atm 96 kg PE·mol^{-1}·h^{-1} with M_w = 16, 000, M_w/M_n = 2.6. Tsukahara, T.; Swenson, D. C.; Jordan, R. F. *Organometallics* **1997**, *16*, 3303−3313. (c) Combinations of $Zr(CH_2Ph)_2$(2,6-bis{menthoxo}pyridyl) with MAO or $B(C_6F_5)_3$ are not active for ethylene polymerization at 20 °C, 1−6 atm; see ref 5.

phenomena, assessing in particular possible transfer of $\{OSO^R\}^{2-}$ ligands between group 4 metal and Al centers. The promising results obtained in this study in terms of coordination/organometallic chemistry and polymerization catalysis suggest possibilities for significant improvement by ligand tuning.

Experimental Section

General Considerations. All manipulations were performed under a purified argon atmosphere using standard high-vacuum Schlenk techniques or in a glovebox. Solvents (toluene, pentane, THF, diethyl ether) were freshly distilled from Na/K alloy under nitrogen and degassed thoroughly by freeze−thaw−vacuum cycles prior to use. Deuterated hydrocarbon solvents (>99.5% D, Eurisotop) were freshly distilled from sodium/potassium amalgam under argon and degassed prior to use. CD_2Cl_2 was distilled from calcium hydride. CD_3CN was dried over 3 and 4 Å molecular sieves. 1-Chloro-2,2-di(4-methylphenyl)-2-ethanol was prepared by reaction of $(4\text{-}MeC_6H_4)MgBr$ with ethyl chloroacetate in THF. Zirconium and titanium precursors $ZrCl_4$, $Zr(OtBu)_4$, $TiCl_4$, and $Ti(OiPr)_4$ were purchased from Aldrich and were used as received. $Zr(CH_2Ph)_4$ was prepared following the literature procedure.[44] $[Ph_3C][B(C_6F_5)_4]$ (Boulder) and MAO (30 wt % solution in toluene, Albermale) were used as received. $B(C_6F_5)_3$ (Boulder) was sublimed twice before use.

NMR spectra of complexes were recorded on Bruker AC-200, AC-300, DRX-400, DRX-500, and AM-500 spectrometers at ambient probe temperature (23 °C) unless otherwise indicated. ^1H and ^{13}C chemical shifts are reported in ppm vs $SiMe_4$ and were determined by reference to the residual solvent peaks. Assignment of signals was made from $^1H-^1H$ COSY, $^1H-^{13}C$ HMQC, and HMBC NMR experiments. ^{19}F NMR spectra are referenced to external neat $CFCl_3$. ^{11}B NMR spectra are referenced to external neat $BF_3{\cdot}OEt_2$. NMR probe temperatures were calibrated by a MeOH thermometer.[45] All coupling constants are given in hertz. Elemental analyses were performed by the Microanalytical Laboratory at the Institute of Chemistry of Rennes and are the average of two independent determinations. Gel permeation chromatography (GPC) was performed on a Polymer Laboratories PL-GPC 220 instrument using 1,2,4-trichlorobenzene solvent (stabilized with 125 ppm BHT) at 150 °C. A set of three PLgel 10 μm mixed-B or mixed-B LS columns was used. Samples were prepared at 160 °C. Polyethylene molecular weights were determined vs polystyrene standards and are reported relative to polyethylene standards, as calculated by the universal calibration method using Mark−Houwink parameters ($K = 14.1 \times 10^{-5}$, $\alpha = 0.70$ for PSt, $K = 14.1 \times 10^{-5}$, $\alpha = 0.70$ for PE).[46] DSC measurements were performed on a TA Instruments DSC 2920 differential scanning calorimeter. Polyethylene samples (10 mg) were annealed by heating to 170 °C at 20 °C/min, followed by cooling to 40 °C at 40 °C/min, then heating to 170 °C at 20 °C/min.

Bis(2-hydroxy-2-methylpropyl)sulfide ($\{OSO^{Me}\}H_2$, 1a). In a 250 mL round-bottom flask, 1-chloro-2-methyl-2-propanol (5.42 g, 50.0 mmol) and $Na_2S{\cdot}9H_2O$ (6.00 g, 25.0 mmol) were refluxed in ethanol (50 mL) for 30 min. The mixture was cooled to room temperature and filtered, and the filtrate was concentrated under vacuum, leaving a white pasty solid. The latter was dissolved in toluene (5 mL) and dried over $MgSO_4$ for 12 h. Filtration, removal of toluene, and drying for 40 h under vacuum gave **1a** as a white crystalline powder (3.20 g, 72%). ^1H NMR ($CDCl_3$, 200 MHz): δ 3.37 (s, 2H, OH), 2.64 (s, 4H, CH_2), 1.18 (s, 12H, CH_3). ^1H NMR (C_6D_6, 200 MHz): δ 3.40 (s, 2H, OH), 2.56 (s, 4H, CH_2), 1.17 (s, 12H, CH_3). ^1H NMR (THF-d_8, 200 MHz): δ 3.94 (s, 2H, OH), 2.65 (s, 4H, CH_2), 1.18 (s, 12H, CH_3). ^1H NMR (pyridine-d_5, 200 MHz): δ 6.01 (s, 2H, OH), 3.00 (s, 4H, CH_2), 1.25 (s, 12H, CH_3). ^1H NMR (CD_3CN, 200 MHz): δ 3.12 (s, 2H, OH), 2.68 (s, 4H, CH_2), 1.20 (s, 12H, CH_3). $^{13}C\{^1H\}$ NMR ($CDCl_3$ and THF-d_8, 50 MHz): δ 71.3 (C), 49.3 (CH_2), 29.1 (CH_3). Anal. Calcd for $C_8H_{18}O_2S$: C, 53.89; H, 10.18; S, 17.98. Found: C, 54.05; H, 10.24; S, 17.85. HRMS: calcd for [M − Me − H_2O] 145.0687, found 145.0666; calcd for [M − Me − 2 H_2O] 127.05815, found 127.0583.

Bis(2,2-di(4-methylphenyl)-2-ethanol)sulfide Hydrate ($\{OSO^{tol}\}H_2{\cdot}H_2O$, 1b). This product was prepared as described above for **1a**, starting from $Na_2S{\cdot}9H_2O$ (2.25 g, 9.40 mmol) and $(4\text{-}MeC_6H_4)_2C(OH)CH_2Cl$ (4.90 g, 18.8 mmol). Addition of pentane (20 mL) to the final red-orange oily residue precipitated **1b** as a colorless powder, which was collected by filtration and dried in a vacuum (34%). Evaporation of the former pentane solution and chromatography of the crude product (silica, heptane/ethyl acetate 100:6 v/v, $R_f = 0.17$) afforded an additional crop of diol (total yield 2.68 g, 57%). ^1H NMR (C_6D_6, 200 MHz): δ 7.38 (d, $^3J_{H-H} = 8.2$ Hz, 8H, $o\text{-}C_6H_4$), 6.96 (d, $^3J_{H-H} = 8.2$ Hz, 8H, $m\text{-}C_6H_4$), 5.11 (s, 2H, H_2O), 3.86 (s, 2H, OH), 3.34 (s, 4H, CH_2), 2.08 (s, 12H, CH_3). $^{13}C\{^1H\}$ NMR (C_6D_6, 50.3 MHz): δ 21.1 (CH_3), 48.4 (CH_2), 78.5 (C_q), 126.8 (*m*-C), 129.3 (*o*-C), 136.8 (*p*-C), 143.8 (*ipso*-C). ^1H NMR (DMSO-d_6, 200 MHz): δ 7.38 (d, $^3J_{H-H} = 8.0$ Hz, 8H, $o\text{-}C_6H_4$), 7.09 (d, $^3J_{H-H} = 8.0$ Hz, 8H, $m\text{-}C_6H_4$), 5.70 (s, 2H, H_2O), 3.47 (s, 4H, CH_2), 2.53 (s, 2H, OH), 2.27 (s, 12H, CH_3). MS(EI): Calcd for [M − 2 H_2O]$^+$ 446.2068, found 446.2093; calcd for [M − H_2O]$^+$ 264.21739, found 264.2113. Anal. Calcd for $C_{32}H_{36}O_3S$: C, 76.78; H, 7.25; S, 6.40. Found: C, 77.25; H, 7.13; S, 6.50.

$K_2\{OSO^{Me}\}$ (2a). Under argon, a solution of **1a** (0.54 g, 3.00 mmol) in THF (20 mL) was added to potassium chunks (0.24 g, 6.2 mmol) in THF (30 mL). The mixture was stirred 4 days at room temperature, resulting in the disappearance of potassium and the formation of a white precipitate. An extra amount of potassium chunks (0.024 g, 0.615 mmol) was added, and the mixture was stirred for two more days. Residual potassium was removed from the mixture, and volatiles were removed under vacuum. The white powder obtained was washed several times with pentane and dried under vacuum (0.73 g, 94%). Anal. Calcd for $C_8H_{16}O_2SK_2$: C, 37.67; H, 6.34; S, 12.60. Found: C, 37.17; H, 6.52; S, 14.02. ^1H NMR (THF-d_8, 200 MHz): δ 2.59 (s, 4H, CH_2), 1.12 (s, 12H, CH_3).

$K_2\{OSO^{tol}\}$ (2b). To a solution of **1b** (0.50 g, 1.00 mmol) in diethyl ether (50 mL) was added KO*t*Bu (0.18 g, 1.60 mmol) at room temperature. The mixture turned red immediately and a precipitate formed. The mixture was stirred for 3 days at room temperature. Filtration of the solution gave **2b** as a colorless precipitate, which was washed with pentane and dried under vacuum (0.146 g, 35%). ^1H NMR (DMSO, 200 MHz): δ 7.22 (d, $^3J_{H-H} = 8.2$ Hz, 8H, $o\text{-}C_6H_4$), 7.00 (d, $^3J_{H-H} = 8.2$ Hz, 8H, $m\text{-}C_6H_4$), 3.30 (s, 4H, CH_2), 2.21 (s, 12H, CH_3). $^{13}C\{^1H\}$ NMR (DMSO, 50.3 MHz): 20.5 (CH_3), 45.9 (CH_2), 77.0 (C_q), 126.0 (*m*-C), 128.1 (*o*-C), 135.1 (*p*-C), 144.7 (*ipso*-C). ^1H NMR (C_6D_6, 200 MHz, low solubility): δ 7.44 (d, $^3J_{H-H} = 8.2$ Hz, 8H, $o\text{-}C_6H_4$), 6.97 (d, $^3J_{H-H} = 8.2$ Hz, 8H, $m\text{-}C_6H_4$), 3.52 (s, 4H, CH_2), 2.11 (s, 12H, CH_3). Anal. Calcd for $C_{32}H_{32}O_2SK_2$: C, 68.77; H, 5.77; S, 5.74. Found: C, 69.2; H, 5.9; S, 5.6.

$\{OSO^{Me}\}(SiMe_3)_2$ (3a). To a solution of **1a** (0.500 g, 2.80 mmol) in toluene (70 mL) were added triethylamine (1.60 mL, 11.8 mmol), DMPA (0.068 g, 0.56 mmol), and $ClSiMe_3$ (1.50 mL, 11.8 mmol). The mixture was stirred for 3 days at room temperature. A heavy precipitate formed, which was removed by filtration. The filtrate was concentrated under vacuum, leaving a white powder, which was washed with pentane (2 × 10 mL) and dried under vacuum (0.78 g, 95%). ^1H NMR (THF-d_8, 200 MHz): δ 2.67 (s, 4H, CH_2), 1.30 (s, 12H, CH_3), 0.12 (s,18H, $Si(CH_3)_3$). ^1H NMR (C_6D_6, 200 MHz): δ 2.66 (s,

(44) Zucchini, U.; Albizzati, E.; Giannini, U. *J. Organomet. Chem.* **1971**, *26*, 357−372.
(45) Van Geet, A. L. *Anal. Chem.* **1970**, *42*, 679−680.
(46) Scholte, Th. G.; Meijerink, N. L. J.; Schofelleers, H. M.; Brands, A. M. G. *J. Appl. Polym. Sci.* **1984**, *29*, 3763−3782.

4H, CH_2), 1.27 (s, 12H, CH_3), 0.16 (s, 18H, $Si(CH_3)_3$). $^{13}C\{^1H\}$ NMR (THF-d_8, 50 MHz): δ 75.3 (C), 49.1 (CH_2), 29.3 (CH_3), 2.8 ($Si(CH_3)_3$). Anal. Calcd for $C_{14}H_{34}O_2SSi_2$: C, 52.11; H, 10.62; S, 9.94. Found: C, 52.24; H, 10.86; S, 9.73.

[OSO^{tol}](SiMe$_3$)$_2$ (3b). To a stirred solution of **1b** (0.53 g, 1.06 mmol) in a 1:1 mixture of toluene and Et_2O (70 mL) was added DBU (0.50 mL, 3.30 mmol) and Me_3SiCl (0.50 mL, 3.90 mmol) at room temperature. A white precipitate formed, and the reaction mixture was stirred for 24 h at 70 °C. The precipitate was filtered off, and volatiles were removed under vacuum. Recrystallization of the residue from pentane at −35 °C gave **3b** as a crystalline beige product (0.41 g, 68%). Anal. Calcd for $C_{36}H_{44}O_2SSi$: C, 76.01; H, 7.80; S, 5.64. Found: C, 76.26; H, 7.94; S, 5.58. ^1H NMR (C_6D_6, 200 MHz): δ 7.30 (d, $^3J_{H-H}$ = 8.0 Hz, 8H, *o*-C_6H_4), 6.98 (d, $^3J_{H-H}$ = 8.0 Hz, 8H, *m*-C_6H_4), 2.90 (s, 4H, CH_2), 2.12 (s, 12H, CH_3), 0.01 (s, 18H, $Si(CH_3)_3$). $^{13}C\{^1H\}$ NMR (C_6D_6, 50.33 MHz): δ 2.3 ($Si(CH_3)_3$), 21.2 (CH_3), 46.7 (CH_2), 81.2 (C_q), 128.2 (*m*-C), 128.7 (*o*-C), 136.7 (*p*-C), 144.7 (*ipso*-C).

Zr(OtBu)$_2${OSO^{Me}} (4). A solution of **1a** (0.100 g, 0.56 mmol) in toluene (3 mL), cooled at −30 °C, was added dropwise over 5 min to a solution of Zr(O*t*Bu)$_4$ (0.215 g, 0.56 mmol) in toluene (2 mL) at −30 °C. The mixture was stirred for 6 h, over which time the temperature was gradually raised to room temperature. Volatiles were removed under vacuum, and the white solid was washed with pentane and dried under vacuum (0.190 g, 91%). Anal. Calcd for $C_{16}H_{34}O_2SZr$: C, 46.45; H, 8.28; S, 7.75. Found: C, 45.95; H, 8.52; S, 6.67. ^1H NMR (THF-d_8, 300 MHz): δ 2.76 (s, 4H, CH_2), 1.26 (s, 18H, *t*Bu), 1.23 (s, 12H, CH_3). $^{13}C\{^1H\}$ NMR (THF-d_8, 75.5 MHz): δ 78.1 ($OC(CH_3)_2$), 73.8 ($C(CH_3)_3$), 53.9 (CH_2), 32.9 ($C(CH_3)_3$), 30.5 ($OC(CH_3)_2$). ^1H NMR (toluene-d_8, 300 MHz, 360 K): δ 2.63 (br s, 4H, CH_2), 1.39 (s, br, 18H, *t*Bu), 1.29 (s, 12H, CH_3). ^1H NMR (toluene-d_8, 300 MHz, −40 °C, assignment made from a COSY experiment): 20 methylene resonances were detected (denoted a−j), δ 4.02 (d, ^2J = 14.5 Hz, 1H, CH_2(a1)), 3.44 (d, ^2J = 12.0 Hz, 1H, CH_2(b1)), 3.31 (d, ^2J = 11.0 Hz, 1H, CH_2(c1)), 3.29 (d, ^2J = 14.5 Hz, 1H, CH_2(a2)), 3.15 (d, ^2J = 14.2 Hz, 1H, CH_2(d1)), 3.13 (d, ^2J = 12.0 Hz, 1H, CH_2(b2)), 3.12 (d, ^2J = 12.8 Hz, 1H, CH_2(e1)), 3.05 (d, ^2J = 14.3 Hz, 1H, CH_2(f1)), 3.02 (d, ^2J = 13.8 Hz, 1H, CH_2(g1)), 2.91 (d, ^2J = 13.0 Hz, 1H, CH_2(h1)), 2.78 (d, ^2J = 11.0 Hz, 1H, CH_2(c2)), 2.62 (d, ^2J = 12.2 Hz, 1H, CH_2(i1)), 2.60 (d, ^2J = 13.0 Hz, 1H, CH_2(h2)), 2.49 (d, 2J = 13.8 Hz, 1H, CH_2(j1)), 2.41 (d, ^2J = 13.8 Hz, 1H, CH_2(g2)), 2.41 (d, ^2J = 13.8 Hz, ^{1}H, CH_2(j2)), 2.37 (d, ^2J = 12.8 Hz, 1H, CH_2(e2)), 2.33 (d, ^2J = 12.2 Hz, 1H, CH_2(i2)), 2.25 (d, ^2J = 14.3 Hz, 1H, CH_2(f2)), 2.24 (d, ^2J = 14.2 Hz, 1H, CH_2(d2)). $^{13}H\{^1H\}$ NMR (toluene-d_8, 125 MHz, −40 °C, selected resonances, assignments made from an HMQC experiment): 10 methylene resonances were detected (denoted a−j), δ 55.3 (CH_2(d)), 54.6 (CH_2(e)), 54.1 (CH_2(f)), 53.1 (CH_2(g)), 47.4 (CH_2(c)), 47.2 (CH_2(b)), 47.1 (CH_2(h)), 47.0 (CH_2(i)), 44.2 (CH_2(j)), 43.2 (CH_2(a)).

Zr{OSO^{Me}}$_2$ (6). This compound was prepared as described above for **4** starting from a solution of **1a** (0.300 g, 1.68 mmol) in toluene (6 mL) and a solution of Zr(O*t*Bu)$_4$ (0.322 g, 0.84 mmol) in toluene (4 mL). Workup gave **6** as a white powder (0.350 g, 92%). Anal. Calcd for $C_{17}H_{36}O_4S_2Zr$: C, 44.41; H, 7.89; S, 13.95. Found: C, 44.81; H, 7.79; S, 14.15. ^1H NMR (thf-d_8, 300 MHz): δ 2.74 (s, 4H, CH_2), 1.20 (s, 12H, CH_3). $^{13}C\{^1H\}$ NMR (THF-d_8, 75.5 MHz): δ 77.1 (OC), 53.8 (CH_2), 29.8 (CH_3). ^1H NMR (toluene-d_8, 300 MHz, 360 K): δ 2.70 (s, 4H, CH_2), 1.29 (s, 12H, CH_3).

Ti{OSOMe}$_2$ (7). Synthesis by Salt Elimination. A yellow suspension of $TiCl_4(Et_2O)$ was prepared by stirring $TiCl_4$ (0.258 g, 1.35 mmol) in diethyl ether (20 mL) at −30 °C for 1 h. Et_3N (1.20 mL, 8.6 mmol) was added by syringe, resulting in the immediate formation of a dark red solution. A solution of **1a** in diethyl ether (10 mL) was then added dropwise at −30 °C, giving an immediate precipitate. The mixture was warmed to room temperature and stirred for 18 h. After filtration of the mixture and concentration of the filtrate under vacuum, a yellow powder was obtained, which was recrystallized from toluene/pentane to give **7** as a white microcrystalline powder (0.287 g, 53%).

Synthesis by Alcohol Elimination. Compound **7** was prepared as described above for **6** starting from a solution of **1a** (0.100 g, 0.56 mmol) in toluene (2 mL) and a solution of Ti(O*i*Pr)$_4$ (0.080 g, 0.28 mmol) in toluene (2 mL) at −30 °C. Workup and recrystallization from pentane at −30 °C gave **7** as a white powder (0.110 g, 81%). Anal. Calcd for $C_{16}H_{32}O_4S_2Ti$: C, 47.99; H, 8.06; S, 16.02. Found: C, 47.78; H, 8.23; S, 15.92. ^1H NMR (C_6D_6, 200 MHz): δ 2.59 (s, 4H, CH_2), 1.23 (s, 12H, CH_3). $^{13}C\{^1H\}$ NMR (C_6D_6, 75.5 MHz): δ 84.1 (OC), 54.0 (CH_2), 29.4 (CH_3). ^1H NMR (THF, 300 MHz): δ 2.75 (s, 4H, CH_2), 1.23 (s, 12H, CH_3). $^{13}C\{^1H\}$ NMR (THF, 75.5 MHz): δ 82.6 (OC), 52.4 (CH_2), 27.7 (CH_3).

Reaction of Ti(O*i*Pr)$_4$ with 1a (1:2 reaction). A solution of Ti(O*i*Pr)$_4$ (0.191 g, 0.67 mmol) in toluene (3 mL) cooled at −30 °C was added dropwise to a cold (−30 °C) solution of ligand **1a** (0.120 g, 0.67 mmol) in toluene. The mixture was warmed to room temperature and stirred for 12 h. Volatiles were removed under vacuum to give a white powder. The ^1H NMR spectrum of this powder in benzene-d_6 displayed two sets of resonances consistent with the presence of both complexes Ti(O*i*Pr)$_2${OSOMe} (**5**, 79%) and Ti{OSOMe}$_2$ (**7**, 21%). Data for Ti(O*i*Pr)$_2${OSOMe}: ^1H NMR (C_6D_6, 500 MHz): δ 4.62 (m, 2H, OC*H*Me$_2$), 2.55 (s, ^{4}H, CH_2), 1.30 (d, $^3J_{H-H}$ = 6.2 Hz, 12H, $CH(CH_3)_2$), 1.21 (s, 12H, CH_3).

Zr(CH$_2$Ph)$_2${OSO^{Me}} (8). Synthesis by Alkane Elimination. A solution of **1a** (0.117 g, 0.658 mmol) in toluene (10 mL) was added at −20 °C to a solution of Zr(CH_2Ph)$_4$ (0.300 g, 0.658 mmol) in toluene (10 mL). The solution was stirred for 2 h at room temperature, and volatiles were removed under vacuum. The brown oily residue was triturated with pentane, and the solid was separated by filtration and dried under vacuum to leave **8** as pale beige powder (0.180 g, 60%). Anal. Calcd for $C_{22}H_{30}O_2SZr$: C, 58.75; H, 6.72; S, 7.13. Found: C, 58.71; H, 6.66; S, 7.06.

Synthesis by Comproportionation. A Teflon-valved NMR tube was charged with Zr(CH_2Ph)$_4$ (0.040 g, 0.088 mmol) and **6** (0.039 g, 0.088 mmol), and toluene-d_8 (ca. 1.5 mL) was vacuum-transferred in at −180 °C. The tube was sealed and warmed to room temperature. ^1H NMR spectroscopy revealed 90% conversion of the starting reagents to **8**. ^1H NMR (toluene-d_8, 300 MHz, 200 K): δ 7.26 (d, ^3J = 7.5 Hz, 2H, *o*-H(b)), 7.17 (m, 2H, *m*-H(b)), 7.09 (m, 2H, *m*-H(a)), 6.93 (m, 2H, *p*-H(a,b)), 6.73 (d, ^3J = 7.5, 2H, *o*-H(a)), 2.67 (d, ^2J = 11.3 Hz, 2H, SCH_2), 2.53 (s, 2H, CH_2Ar(a)), 1.82 (d, ^2J = 11.3 Hz, 2H, SCH_2), 1.75 (s, 2H, CH_2Ar(b)), 1.17 (s, 12H, CH_3). ^1H NMR (toluene-d_8, 300 MHz, 333 K): δ 7.08−6.80 (m, 10H, Ph), 2.34 (s, 4H, CH_2), 2.05 (s, 4H, CH_2), 1.06 (s, 12H, CH_3). ^{13}C NMR (toluene-d_8, 75.5 MHz, 200 K): δ 147.6 (*ipso*-C(b)), 136.5 (*ipso*-C(a)), 131.6 (*m*-C(a)), 129.0 (*o*-C(b)), 128.1 (*m*-C(b)), 127.3 (*o*-C(a)), 128.1 (*m*−C(b)), 122.7 (*p*-C(a)), 119.7 (*p*-C(b)), 84.2 (s, OC), 54.9 (t, J_{C-H} = 139.3 Hz, SCH_2), 54.9 (t, J_{C-H} = 139.3 Hz, CH_2Ar(a)), 53.6 (t, J_{C-H} = 128.5 Hz, CH_2Ar(b)), 30.1 (q, J_{C-H} = 123.7 Hz, CH_3), 29.4 (q, J_{C-H} = 126.3, CH_3). $^{13}C\{^1H\}$ NMR (toluene-d_8, 75.5 MHz, 293 K): δ 137.5 (Ph), 130.3 (Ph), 122.2 (Ph), 84.3 (OC), 55.8 (CH_2), 55.4 (CH_2), 29.9 (CH_3).

ZrCl$_2${OSOMe} (9). Synthesis by Alkane Elimination. To a vigorously stirred solution of $ZrCl_4$ (0.500 g, 2.15 mmol) in toluene (15 mL) cooled at −78 °C was added dropwise *n*BuLi (2.7 mL of a 1.6 M solution in hexanes, 4.30 mmol) over 1 h. The mixture was gently warmed to room temperature and stirred for 8 h, resulting in the formation of a dark brown suspension of "$ZrBu_2Cl_2$ + 2 LiCl". The mixture was cooled to −40 °C, and a solution of **1a** (0.383 g, 2.15 mmol) in toluene (5 mL) was added dropwise over 30 min. The reaction mixture was stirred for 2 h at −40 °C and an additional 8 h period at room temperature. Gas evolution (butane) was noticed without significant change of the color. The precipitate (LiCl) was

removed by filtration and washed with toluene, and the filtrate was concentrated under vacuum to leave **9** as a white powder (0.350 g, 47%). Anal. Calcd for $C_8H_{16}Cl_2O_2SZr$: C, 28.39; H, 4.77; S, 9.48. Found: C, 28.74; H, 5.12; S, 9.26. ^{1}H NMR (THF-d_8) showed resonances only for **11a-*d*$_{16}$.**

Synthesis by Comproportionation of 6 and $ZrCl_4$. A solution of **6** (0.068 g, 0.135 mmol) in toluene (5 mL), cooled at −30 °C, was added to a suspension of $ZrCl_4$ (0.036 g, 0.135 mmol) in toluene (5 mL) placed at −30 °C. The mixture was stirred for 12 h with slow warming to room temperature. Removal of volatiles under vacuum left **9** as a white powder (0.091 g, 100%). ^{1}H NMR (THF-d_8) showed resonances for **11a** (95%) and **11b** (5%).

$ZrCl_2${OSO^{Me}}(THF) (10). (a) One-Pot Synthesis from 1a. To a solution of **1a** (1.00 g, 5.6 mmol) in THF (25 mL) cooled at −78 °C was added dropwise *n*BuLi (7.0 mL of a 1.6 M solution in hexanes, 11.0 mmol). The reaction mixture was gently warmed to room temperature and stirred for 2 h. The clear solution was then cooled to −40 °C and transferred via cannula over 30 min onto a suspension of $ZrCl_4$ (1.31 g, 5.6 mmol) in THF (25 mL) at −40 °C. The solution, which progressively turned yellow upon addition of the dialkoxide, was stirred for 20 h at room temperature, and THF was removed under vacuum. The residue was extracted with toluene (4 × 25 mL), and the solution was filtered through a Celite pad and concentrated under vacuum to leave **10** as a white powder (1.65 g, 61%).

(b) Synthesis from Dipotassium Salt 2a. A suspension of $ZrCl_4$ (0.210 g, 0.90 mmol) in THF (10 mL) cooled at −35 °C (prepared 1 h before use) was added under stirring to K_2{OSO^{Me}} (**2a**) (0.229 g, 0.90 mmol) placed in a Schlenk flask. The mixture was warmed to room temperature and stirred for 24 h. The solution was filtered to remove the precipitate (KCl) and concentrated under vacuum. The beige residue was extracted with toluene (3 × 10 mL), and the solution was filtered through a Celite pad and concentrated under vacuum. The residue was washed with pentane (2 × 3 mL) and dried under vacuum to leave **10** as a white powder (0.170 g, 55%). Anal. Calcd for $C_{12}H_{24}O_3SCl_2Zr$: C, 35.11; H, 5.89; S, 7.81. Found: C, 35.08; H, 6.08; S, 7.60. ^{1}H NMR (CD_3CN, 200 MHz): δ 3.80 (m, 4H, THF), 2.66 (s, 4H, CH_2), 1.25 (m, 4H, THF), 1.17 (s, 12H, CH_3). The ^{13}C NMR spectrum in THF-d_8 was as described below for **11**.

$ZrCl_2${OSO^{Me}}$(THF)_2$ (11). Complex **11** was obtained by recrystallization of **10** in THF at −30 °C. The crystals were separated from the solution, washed with pentane, and dried under partial vacuum. Anal. Calcd for $C_{16}H_{32}Cl_2O_4SZr$: C, 39.82; H, 6.68; S, 6.64. Found: C, 40.13; H, 6.78; S, 6.59. ^{1}H NMR (CD_3CN, 200 MHz): δ 3.80 (m, 8H, THF), 2.66 (s, 4H, CH_2), 1.25 (m, 8H, THF), 1.17 (s, 12H, Me). Two series of resonances are observed in THF, assigned to two isomers, **11a** (89−91%) and **11b** (9−11%). **11a** ^{1}H NMR (THF-d_8, 200 MHz): δ 2.78 (s, 4H, CH_2), 1.23 (s, 12H, Me). ^{13}C{^{1}H} NMR (THF-d_8, 50 MHz): δ 81.1 (OC), 53.1 (s, CH_2), 29.1 (CH_3). **11b** ^{1}H NMR (THF-d_8, 200 MHz): δ 2.65 (s, 4H, CH_2), 1.18 (s, 12H, CH_3). ^{13}C{^{1}H} NMR (THF-d_8, 50 MHz): δ 70.8 (OC), 49.2 (CH_2), 29.1 (CH_3).

$TiCl_2${OSO^{Me}} (12). $TiCl_4$ (0.090 g, 0.48 mmol) was added dropwise to a solution of Ti(O*i*Pr)$_4$ (0.136 g, 0.48 mmol) in toluene (2 mL) at room temperature. The mixture was stirred for 1 h. A solution of **1a** (0.170 g, 0.96 mmol) in toluene (3 mL), cooled at −30 °C, was added to the previous mixture over 2 min, and the mixture was stirred for 12 h. Removal of volatiles under vacuum, washing of the solid residue with pentane, and drying at room temperature gave **12** as a white powder (0.230 g, 82%). Anal. Calcd for $C_8H_{16}O_2STiCl_2$: C, 32.57; H, 5.47; S, 10.87. Found: C, 32.31; H, 5.65; S, 9.65. ^{1}H NMR (C_6D_6, 200 MHz): δ 2.37 (s, 4H, CH_2), 1.00 (s, 12H, CH_3). ^{13}C{^{1}H} NMR (C_6D_6, 50 MHz): δ 95.9 (OC), 53.9 (CH_2), 28.8 (CH_3). ^{1}H NMR (toluene-d_8, 500 MHz, −55 °C) (assignments made from HMBC, HMQC, and COSY experiments): δ 4.27 (d, ^2J = 12.3 Hz, ^{1}H, CH_2(a1)), 4.05 (d, $2J$ = 10.5 Hz, 1H, CH_2(b1)), 3.92 (d, ^2J = 13.8 Hz, 1H, CH_2(c1)), 3.77 (d, ^2J = 12.3 Hz, 1H, CH_2(a2)), 3.50 (d, ^2J = 13.8 Hz, 1H, CH_2(c2)), 3.46 (d, ^2J = 15.9 Hz, 1H, CH_2(d1)), 1.92 (d, ^2J = 15.9 Hz, 1H, CH_2(d2)), 1.74 (d, ^2J = 10.5 Hz, 1H, CH_2(b2)), 1.84 (s, 3H, CH_3(a3)), 1.64 (s, 3H, CH_3(a4)), 1.53 (s, 3H, CH_3(b3)), 1.47 (s, 3H, CH_3(c3)), 1.26 (s, 3H, CH_3(b4)), 1.21 (s, 3H, CH_3(d3)), 1.11 (s, 3H, CH_3(c4)), 1.08 (s, 3H, CH_3(d4)). ^{13}C{^{1}H} NMR (toluene-d_8, 125 MHz): δ 96.1 (C(c)), 96.0 (C(d)), 92.6 (C(a)), 91.1 (C(b)), 53.7 (CH_2(c)), 51.8 (CH_2(a)), 49.5 (CH_2(b)), 48.7 (CH_2(d)), 29.6 (CH_3(d3)), 28.9 (CH_3(a3), CH_3(b3), CH_3(c4), CH_3(d4)), 27.4 (CH_3(a4)), 26.9 (CH_3(c3)), 26.3 (CH_3(b4)).

$TiCl_2${OSO^{Me}}$(THF)_2$ (13). Synthesis by Salt Elimination. *n*-Butyllithium (12.4 mL of a 1.6 M solution in *n*-hexane, 20.0 mmol) was added dropwise at −20 °C to a solution of **1a** (1.61 g, 9.0 mmol) in THF (25 mL). The mixture was stirred at room temperature for 2 h, then cooled to −35 °C, and slowly transferred over 30 min into a solution of $TiCl_4$ (1.72 g, 9.0 mmol) in THF (20 mL) at −35 °C (prepared 5 h before). The solution, which turned orange upon adding the dialkoxide, was stirred for 30 h at room temperature and then concentrated under vacuum until obtaining an oily residue. The residue was washed with pentane (2 × 10 mL) and extracted with toluene (2 × 10 mL). Toluene was evaporated under vacuum to give an orange oily residue, which was triturated with pentane for 12 h. The white precipitate was removed by filtration, and the filtrate was concentrated under vacuum to give **13** as a white solid (1.22 g, 45%). Complex **13** was also obtained by recrystallization of **12** in THF at −30 °C. Anal. Calcd for $C_{16}H_{32}Cl_2O_4STi$: C, 43.75; H, 7.34; S, 7.30. Found: C, 44.14; H, 7.42; S, 7.15. ^{1}H NMR (THF-d_8, 200 MHz): δ 2.94 (s, 4H, CH_2), 1.29 (s, 12H, CH_3). ^{13}C{^{1}H} NMR (THF-d_8, 75.5 MHz): δ 83.1 (OC), 50.8 (CH_2), 31.4 (CH_3).

Reaction of $TiCl_4$ and 1b. Generation of "$TiCl_2$-{OSO^{tol}}" (14). A solution of **1b** (0.441 g, 0.88 mmol) in toluene (20 mL) was added dropwise at 0 °C to a stirred solution of $TiCl_4$ (0.258 g, 1.35 mmol) in pentane (20 mL). A yellow-green precipitate rapidly formed. The mixture was stirred for 20 h at room temperature. The solid was collected by filtration, washed with pentane (3 × 5 mL), and dried under vacuum, leaving a yellow powder (0.358 g, 66%). This product was insoluble in C_6D_6. ^{1}H NMR (THF-d_8, 200 MHz): δ 6.5−7.2 (16H, H aro), 3.36 (s, 4H, CH_2), 2.28 (s, 12H, CH_3). ^{13}C{^{1}H} NMR (THF-d_8, 50 MHz): δ 125.0−143.0 (C_{aro}), 45.0 (CH_2), 18.8 and 18.6 (CH_3) (C_q not observed). Anal. Calcd for $C_{32}H_{32}O_2Cl_2STi$: C, 64.12; H, 5.38; S, 5.35. Found: C, 60.45; H, 5.28; S, 4.73. Repeated elemental analyses on materials from different batches gave systematically poor results, indicating contamination of **14** with unidentified impurities.

Reaction of $Zr(CH_2Ph)_2${OSO^{Me}} (8) with $[Ph_3C][B(C_6F_5)_4]$. Generation of $[Zr(CH_2Ph)${OSO^{Me}}$][B(C_6F_5)_4]$ (15). A Teflon-valved NMR tube was charged with $Zr(CH_2Ph)_2${OSO^{Me}} (**8**, 0.012 g, 0.026 mmol) and $[Ph_3C][B(C_6F_5)_4]$ (0.024 g, 0.026 mmol), and CD_2Cl_2 (0.6 mL) was a vacuum transferred at −180 °C. The tube was sealed and kept at −80 °C. A yellow solution formed within 5 min. The ^{1}H NMR spectrum was recorded at −33 °C and indicated that **15** had formed quantitatively. Compound **15** is not soluble in hydrocarbons (toluene, pentane, hexanes). NMR assignments were made from 2D HMBC, HMQC, and COSY experiments. ^{1}H NMR (CD_2Cl_2, 500 MHz, 240 K): δ 8.30 (t, ^3J = 7.7 Hz, 1H, *p*-H(ZrBz), 7.91 (t, ^3J = 7.8 Hz, 2H, *m*-H(ZrBz), 7.69 (d, ^3J = 7.6 Hz, 2H, *o*-H(ZrBz), 3.70 (d, ^2J = 13.2 Hz, 1H, SCH_2), 3.45 (d, ^2J = 13.2 Hz, 1H, SCH_2), 3.32 (d, ^2J = 13.7 Hz, 1H, SCH_2), 3.24 (d, ^2J = 9.4 Hz, 1H, $ZrCH_2$), 3.05 (d, ^2J = 9.4 Hz, 1H, $ZrCH_2$), 2.95 (d, ^2J = 13.7 Hz, 1H, SCH_2), 1.74 (s, Me), 1.42 (s, Me), 1.33 (s, Me), 1.22 (s, Me). ^{13}C{^{1}H} NMR (CD_2Cl_2, 100 MHz, 240 K): δ 148.1 (dm, J_{C-F} = 240 Hz, *o*-C_6F_5), 142.9 (*p*-C(ZrBz)), 142.0 (*o*-C(ZrBz)), 138.0 (dm, J_{C-F} = 244 Hz, *p*-C_6F_5), 136.2 (dm, J_{C-F} = 248 Hz, *m*-C_6F_5), 132.4 (*ipso*-

C(ZrBz)), 131.1 (*m*-C(ZrBz)), 92.4 (SCH_2CMe_2), 91.9 (SCH_2CMe_2), 74.5 ($ZrCH_2Ph$), 59.9 (SCH_2), 51.3 (SCH_2), 31.4 (CH_3), 29.8 (CH_3), 29.2 (CH_3), 28.1 (CH_3). ^{11}B NMR (CD_2Cl_2, 128 MHz, 240 K): δ −15.8 (br s, $B(C_6F_5)_4^-$). $^{19}F\{^1H\}$ NMR (CD_2Cl_2, 376 MHz, 240 K): δ −132.1 (d, $^3J_{F-F}$ = 19.3 Hz, 8F, *o*-F $B(C_6F_5)_4^-$), −162.3 (t, $^3J_{F-F}$ = 19.3 Hz, 4F, *p*-F $B(C_6F_5)_4^-$), −166.2 (t, $^3J_{F-F}$ = 19.3 Hz, 8F, *m*-F $B(C_6F_5)_4^-$). ^1H resonances for Ph_3CCH_2Ph:[32] δ 7.30 (m, 12H, *o*-H and *m*-H(CPh_3)), 7.27 (m, 3H, *p*-H(CPh_3)), 7.12 (t, ^3J = 7.7 Hz, 1H, *p*-H(Bz)), 7.03 (t, ^3J = 7.5 Hz, 2H, *m*-H(Bz)), 6.68 (d, ^3J = 7.5 Hz, 2H, *o*-H(Bz)), 3.92 (s, 2H, CH_2(Bz)). ^{13}C NMR: δ 146.6 (*ipso*-C(CPh_3)), 138.4 (*ipso*-(Bz), 131.1 (*o*-C(Bz)), 129.6 (*o*-C(CPh_3)), 127.5 (*m*-C(CPh_3)), 127.8 (*m*-C(Bz)), 126.0 (p−C(Bz and CPh_3)), 58.5 (CPh_3CH_2Ph), 45.6 (CPh_3CH_2Ph).

Reaction of $Zr(CH_2Ph)_2\{OSOMe\}$ (8) with $B(C_6F_5)_3$. Generation of $[Zr(CH_2Ph)\{OSOMe\}][PhCH_2B(C_6F_5)_3]$ (16). A Teflon-valved NMR tube was charged with $Zr(CH_2Ph)_2\{OSO^{Me}\}$ (**8**, 0.015 g, 0.033 mmol) and $B(C_6F_5)_3$ (0.017 g, 0.033 mmol), and toluene-d_8 (0.6 mL) was vacuum transferred in at −180 °C. The tube was sealed and kept at −80 °C. A yellow solution formed within 5 min. The ^1H NMR spectrum was recorded at −33 °C and indicated that **16** was formed in 90% yield. ^1H NMR (toluene-d_8, 400 MHz, 240 K): δ 7.24−6.78 (br m, 8H), 6.15 (br m, 2H), 3.47 (s, br, 2H, BCH_2Ph), 2.38 (d, ^2J = 11.8 Hz, 2H, SCH_2), 2.25 (s, 2H, $ZrCH_2Ph$), 1.25 (d, ^2J = 11.8 Hz, 2H, SCH_2), 0.82 (s, 6H, CH_3), 0.76 (s, 6H, CH_3). ^1H NMR (toluene-d_8, 400 MHz, 298 K): δ 7.01 (m, 2H, *m*-H BBz), 6.95 (d, ^3J = 8.5 Hz, 2H, *o*-H BBz), 6.79 (m, 1H, *p*-H BBz), 6.74 (d, ^3J = 7.4 Hz, 2H, *o*-H ZrBz), 6.20 (m,2H, *m*-H ZrBz), 6.11 (m, 1H, *p*-H ZrBz), 3.38 (br s, 2H, BCH_2Ph), 2.34 (br m, 2H, SCH_2), 2.17 (s, 2H, $ZrCH_2Ph$), 1.58 (br m, 2H, SCH_2), 0.82 (s, 12H, CH_3). $^{13}C\{^1H\}$ NMR (toluene-d_8, 100 MHz, 240K): δ 159.2 (*ipso*-BBz), 149.6 (br d, J_{C-F} = 242 Hz, *o*-C_6F_5), 140.0 (*ipso*-ZrBz), 139.6 (br d, J_{C-F} = 243 Hz, *p*-C_6F_5), 138.2 (br d, J_{C-F} = 245 Hz, *m*-C_6F_5), 130.8−126.1 (*o*-BBz, *m*-BBz, *o*-ZrBz, *m*-ZrBz), 126.0−123.3 (*p*-ZrBz, *p*-BBz), 87.6 (C), 65.3 ($ZrCH_2Ph$), 54.3 (2C, SCH_2), 29.2 (2C, CH_3), 28.3 (2C, CH_3). ^{11}B NMR (toluene-d_8, 128 MHz, 240 K): δ −11.4 (br s, $\{B(C_6F_5)_3Bz\}^-$). $^{19}F\{^1H\}$ NMR (toluene-d_8, 376 MHz, 240 K): δ −130.0 (br m, 6F, *o*-F $\{B(C_6F_5)_3Bz\}^-$), −159.8 (t, $3J_{F-F}$ = 19.8 Hz, 3F, *p*-F $\{B(C_6F_5)_3Bz\}^-$), −163.5 (t, $3J_{F-F}$ = 19.8 Hz, 6F, *m*-F $\{B(C_6F_5)_3Bz\}^-$).

Compound **16** slowly decomposes at room temperature within 24 h to form **17**, formulated $[Zr(C_6F_5)\{OSO^{Me}\}][B(CH_2Ph)_2(C_6F_5)_3]$ (assignments made from 2D-HMBC, HMQC, and COSY NMR experiments). ^1H NMR (toluene-d_8, 400 MHz): δ 7.15 (d, ^2J = 7.6 Hz, 2H, *o*-H η^6-BzB), 7.01 (t, ^2J = 7.1 Hz, 2H, *m*-H BzB) and 6.98 (t, ^2J = 7.5 Hz, 1H, *p*-H BzB) (overlap with toluene resonances), 6.77 (d, ^2J = 7.1 Hz, 2H, *o*-H BzB), 6.25 (t, ^2J = 7.6 Hz, 2H, *m*-H η^6-BzB), 6.08 (t, ^2J = 7.1 Hz, 1H, *p*-H η^6-BzB), 3.45 (br m, 2H, CH_2 η^6-BBz), 2.88 (s, 2H, CH_2 BBz), 2.27 (s, 4H, SCH_2), 1.01 (s, 6H, CH_3), 0.84 (s, 6H, CH_3). $^{13}C\{^1H\}$ NMR (toluene-d_8, 100 MHz): δ 161.5 (*ipso*-η^6-BzB), 149.6 (d, ^2J = 244 Hz, *o*-BC_6F_5), 139.8 (d, ^2J = 245 Hz, *p*-BC_6F_5), 139.1 (d, ^2J = 248 Hz, *m*-BC_6F_5), 137.1 (*ipso*-BzB), 132.6 (*o*-η^6-BzB), 131.5 (*p*-η^6-BzB), 129.1 (*o*-BzB), 128.5 (*m*-BzB), 126.0 (*p*-BzB), 125.3 (*p*-η^6-BzB), 90.1 (CMe_2), 50.9 (SCH_2), 38.2 (CH_2 BBz), 35.9 (br, CH_2 η^6-BBz), 31.2 (CH_3), 31.3 (CH_3); resonances for Zr−C_6F_5 were not observed. ^{11}B NMR (toluene-d_8, 128 MHz): δ −11.7 (br s, $\{B(C_6F_5)_2Bz_2\}^-$). ^{19}F NMR (toluene-d_8, 376 MHz): −114.9 (dm, ^3J = 34 Hz, *o*-F ZrC_6F_5), −130.4 (d, ^3J = 24 Hz, *o*-F BC_6F_5), −131.9 (dm, ^3J = 25 Hz, *o*-F ZrC_6F_5)), −158.0 (m, *p*-F ZrC_6F_5), −160.0 (t, ^3J = 20 Hz, *p*-F BC_6F_5), −160.3 (m, *m*-F ZrC_6F_5), −161.0 (m, *m*-F ZrC_6F_5), −164.1 (t, ^3J = 20 Hz, *m*-F BC_6F_5).

Crystal Structure Determination of Ligand Derivatives 1b and 3b and Complexes 4, 7, 11, and 13. Suitable single crystals were mounted onto glass fibers using the "oil-drop" method. Diffraction data were collected at 100−120 K or 279−293 K using a NONIUS Kappa CCD diffractometer with graphite-monochromatized Mo Kα radiation (λ = 0.71073 Å). A combination of ω- and φ-scans was carried out to obtain at least a unique data set. Crystal structures were solved by means of the Patterson method; remaining atoms were located from difference Fourier synthesis, followed by full-matrix least-squares refinement based on F^2 (programs SHELXS-97 and SHELXL-97).[47] Many hydrogen atoms could be found from the Fourier difference. Carbon-bound hydrogen atoms were placed at calculated positions and forced to ride on the attached carbon atom. The hydrogen atom contributions were calculated but not refined. All non-hydrogen atoms were refined with anisotropic displacement parameters. The locations of the largest peaks in the final difference Fourier map calculation as well as the magnitude of the residual electron densities were of no chemical significance. The crystal structure of **3b** belongs to the non-centrosymmetric space group *C*2 (centrosymmetric space groups such as *C*2/*c* were found inappropriate), due to the presence in the elementary cell of two molecules that slightly differ in the conformation of the *p*-tolyl groups. The crystal structure of molecule **4b** is characterized by a complicated disorder model, which involves the simultaneous presence of *tert*-butoxide and chelating thioether ligands at the same position of the ligand sphere. Crystal data and details of data collection and structure refinement for the different compounds are given in Table 1. Crystallographic data are also available as cif files (see Supporting Information Available).

Line-Shape Analysis and NMR Simulations. NMR spectral simulations for **8** were performed using "gNMR" (Cherwell Scientific). Simulations of the NC*HH*CMe_2 and ZrC*HH*Ph hydrogens were performed in a two-step procedure. First, the chemical shifts observed in the slow limit exchange (below 215 K) were used to set up the spin systems. The relative population ratio was fixed at 1:1:1:1 (mole fraction of each site = 0.25). The natural line-width in the absence of exchange W_0 = 0.8 Hz was measured for the Me hydrogens at 210 K. The chemical shifts of the NC*HH*CMe_2 and ZrC*HH*Ph hydrogens vary slightly in the slow limit exchange, and a linear extrapolation was used to estimate the chemical shifts at higher temperatures. We checked that the observed and calculated chemical shifts for the collapsed resonances are identical. Then, for nine temperatures in the range 213 to 333 K, the exchange rate was varied to get the best fit between the simulated and the experimental spectra. Activation parameters were determined by a standard Eyring analysis, and the standard deviations from the least-squares fit were used to estimate the uncertainties in $\Delta H^{\ddagger}$ and $\Delta S^{\ddagger}$.[48]

Ethylene Polymerization. Polymerization experiments (Table 5) were performed in a 150 or 320 mL high-pressure glass reactor equipped with a mechanical stirrer and externally heated with a double mantle with a circulating oil bath as desired. In a typical experiment, the reactor was filled with toluene (25 or 70 mL, depending on the size of the reactor) and MAO (30 wt % solution in toluene, 2−3 or 6−8 mL, 500 equiv) or Al*i*Bu_3 (0.5−0.8 mL, 10 equiv) and pressurized at 5 atm of ethylene (Air Liquide, 99.99%). The reactor was thermally equilibrated at the desired temperature for 1 h. Ethylene pressure was decreased to 1 atm, and the catalyst precursor (30−50 or 120−150 μmol) in toluene (5 or 10 mL) was added by syringe. The ethylene pressure was immediately increased to 5 atm, and the solution was stirred for the desired time. Ethylene consumption was monitored using an electronic manometer connected to a secondary 100 mL ethylene tank,

(47) (a) Sheldrick, G. M. *SHELXS-97*, Program for the Determination of Crystal Structures; University of Goettingen: Germany, 1997. (b) Sheldrick, G. M. *SHELXL-97*, Program for the Refinement of Crystal Structures; University of Goettingen: Germany, 1997.

(48) (a) Bevington, P. R. *Data Reduction and Error Analysis for the Physical Sciences*; McGraw-Hill: New York, 1969. (b) Skoog, D. A.; Leary, J. J. *Principles of Instrumental Analysis*, 4th ed.; Saunders College, 1992; pp 13−14.

which feeds the reactor by maintaining constant the total pressure. The polymerization was stopped by venting of the vessel and quenching with a 10% HCl solution in methanol (30 or 80 mL). The polymer was collected by filtration, washed with methanol and acetone (2 × 20 mL), and dried under vacuum overnight.

Melting temperatures of PE samples were determined on a Perkin-Elmer Pyris 1 differential scanning calorimeter (10 °C/min, nitrogen flow, second pass). Gel permeation chromatography (GPC) analyses were performed on a Polymer Laboratories PL-GPC 220 instrument using 1,2,4-trichlorobenzene as solvent (stabilized with 125 ppm BHT) at 150 °C. A set of three PLgel 10 μm mixed-B or mixed-B LS columns was used. Samples were prepared at 160 °C and filtered through 2 or 5 μm stainless steel frits prior to injection. Molecular weights were determined vs polystyrene standards and are reported relative to polyethylene standards, as calculated by the universal calibration method using Mark−Houwink parameters ($K = 17.5 \times 10^{-5}$, $\alpha = 0.670$ for polystyrene; $K = 40.6 \times 10^{-5}$, $\alpha = 0.725$ for polyethylene).

Acknowledgment. This work was supported by the Ministère de la Recherche et de l'Enseignement Supérieur (Ph.D. grant to L.L.) and the Centre National de la Recherche Scientifique (post-doc fellowship to A.S., ATIPE fellowship to J.F.C.). Work at the University of Chicago was supported by the U.S. Department of Energy (DE-FG02-00ER15036). We thank Dr. Christian W. Lehmann (Max Planck Institut, Mülheim an der Ruhr, Germany) for the X-ray crystal diffraction analysis of **4**.

Supporting Information Available: Crystallographic data for **1b**, **3b**, **4**, **7**, **11**, and **13** as CIF files; additional NMR data (HMQC/HMBC/COSY; VT ^{1}H NMR) for complexes **8**, **15**, **16**, and **17** (^{11}B monitoring); representative GPC traces and DSC profiles of PEs prepared. This material is available free of charge via the Internet at http://pubs.acs.org

OM050560C